Supporting Information

Non-covalent graphene nanobuds from mono- and tripodal binding motifs

Marina Garrido,[§a] Joaquín Calbo,[§b] Laura Rodríguez-Pérez,[a] Juan Aragó,[b] Enrique Ortí,[*b] Mª Ángeles Herranz[*a] and Nazario Martín[*ac]

[a] *Departamento de Química Orgánica I, Facultad de Química, Universidad Complutense de Madrid, Avda. Complutense s/n, 28040 Madrid, Spain. E-mail: maherran@ucm.es, nazmar@ucm.es*

[b] *Instituto de Ciencia Molecular, Universidad de Valencia, 46980 Paterna, Spain. E-mail: enrique.orti@uv.es*

[c] *IMDEA-Nanociencia, c/Faraday 9, Campus Cantoblanco, 28049 Madrid, Spain*

[§] These authors contributed equally

Experimental Section

Supplementary Figures

S18. Evolution of the pyrene–C_{60} and C_{60}–graphene distances in **1**·graphene along the 400 ns MM/MD simulation in solution.

S19. Evolution of the tilting angle θ in **2**·graphene along the 800 ns MM/MD simulation in solution starting from a C_{60}–graphene interacting conformation.

S20. Representative structures of **2**·graphene along the 800 ns MM/MD simulation in solution starting from a C_{60}–graphene interacting conformation.

S21. Evolution of the tilting angle θ in **2**·graphene along the 800 ns MM/MD simulation in solution starting from a C_{60}–graphene non-interacting conformation.

S22. Evolution of the distance between pristine C_{60} and graphene along the 160 ns MM/MD simulation in solution.

Experimental Section

1. Materials and methods

The graphite used for graphene exfoliation was purchased from TIMCAL (TIMREX SFG15, ρ = 2.26 g·cm^{-3}, particle size = 8.80 μm, surface area = 9.50 m^2·g^{-1} ash ≤ 0.100%, interlaminar distance = 0.3354–0.3358 nm). Graphite (0.2 g) was dispersed in *N*-methylpyrrolidone (NMP) (100 mL) and sonicated at room temperature during 150 minutes in a low-power sonication bath, to obtain homogeneous aggregates. This dispersion was then centrifuged at 500 rpm for 45 minutes. After this process, the supernatant was isolated on vials with a Pasteur pipette. The FLG dispersion was kept in solution for further reactions.

All reagents were purchased from commercial sources and used without further purification unless otherwise stated. Thin-layer chromatography was performed on Merck silica gel 60 F254 plates; chromatograms were visualized with UV light (254 and 360 nm). Flash column chromatography was performed on Merck silica gel 60 (ASTM 230-400 mesh). Vacuum filtrations of graphene materials were carried out with polytetrafluoroethylene (PTFE) (pore size = 0.2 μm, Φ = 47 cm) membranes.

2. Instruments

^{1}H NMR and ^{13}C NMR spectra were recorded at 300 and 75 MHz (Varian Mercury-300 instrument), 500 and 125 MHz (Varian Inova 500) or 700 and 175 MHz (Bruker AVIII 700 MHz), respectively. Mass spectra were realized by the mass spectra services at the Universidad Complutense de Madrid. Electronic Impact measurements (EI) were recorded using a HP 5989A apparatus (70 eV, 200 ºC). MALDI-TOF measurements were recorded utilizing a Brucker Ultraflex III apparatus. UV-Vis-NIR spectra were recorded with a Shimadzu Spectrophotometer UV-3600 at 298 K, with a resolution of 1 nm. FTIR spectra were carried out in a Bruker TENSOR 27 using a spectral range of 4000–400 cm^{-1}, with a resolution of 1 cm^{-1}, and in pellets of dispersed samples of the corresponding materials in dried KBr. TGA analyses were carried out under nitrogen in a TA-TGA-Q500 apparatus. The sample (~ 0.5 mg) was introduced inside a platinum crucible and equilibrated at 100 ºC followed by a 10 °C min^{-1} ramp between 100 and 1000 °C followed by an isotherm of 30 minutes. Raman spectra were recorded on a NT-MDT-in Via Microscope at room temperature using an exciting laser source of 532 nm. TEM micrographs were obtained using a JEOL 2100 microscope operating at 200 kV. The samples were dispersed in NMP and dropped onto a holey carbon copper grid (200 mesh), the solvent was removed in a vacuum oven during 48 h. AFM was performed under ambient conditions using SPM Nanoscope IIIa multimode working on tapping mode with a RTESPA tip (Veeco) at a working frequency of B235 KHz. Height and phase images were simultaneously obtained. The samples were prepared by drop-casting or spin coating on freshly cleaved mica and were dried under ambient conditions for 24 hours and later in a vacuum oven during 48 hours. SEM was performed on a JEOL JSM 6335F, working at 10 kV. Samples were deposited by drop-casting on a glass plate, dried in a vacuum oven during 48 hours and metallized with Au prior to observation. Confocal microscopy was performed under ambient conditions on an OLYMPUS FV1200, with three confocal detectors and seven lasers. The samples were prepared by drop-casting on a glass plate and measured with an exciting laser source of 405 nm.

3. Theoretical Calculations

In order to shed light into the supramolecular recognition of the monopodal and tripodal pyrene-based derivatives by graphene, a comprehensive theoretical analysis was performed using molecular mechanics calculations by means of the general MM3 force field[1] using Tinker 7.1.[2] Long molecular dynamics simulations were carried out for the supramolecular assembly of **1** and **2** with a graphene monolayer large enough to bear the bigger tripodal derivative. First, the geometry of the graphene sheet was optimized in vacuum at the MM3 level with terminal hydrogen atoms. Then, the pyrene-based derivatives **1** and **2** were placed over the graphene sheet and their minimum-energy geometries obtained while keeping frozen the graphene sheet atoms. The dynamics simulations were performed in vacuum, without periodic conditions and at room temperature (298 K) during 10 ns with a time step of 1 fs. The graphene sheet was frozen during all the simulation. Characteristic intramolecular geometry parameters (Figure S14) for the pyrene derivatives are analyzed during the dynamics (Figure S15 and S16) to better understand the supramolecular recognition along time. The non-covalent forces stabilizing the resulting nanohybrids are gathered in Figure S17.

Molecular dynamics simulations in solution were performed using the NAMD software[3] including a box of explicit chloroform molecules as a representative organic solvent. The temperature and pressure were maintained at 298 K and 101.325 kPa (1 atm), respectively, by the Langevin thermostat and Langevin piston methods.[4] Non-bonded interactions were calculated using a scaled 1–4 protocol, in which all 1–3 pairs are excluded and all pairs that match the 1–4 criteria are modified. The electrostatic interactions for such pairs are modified by the constant factor defined by 1–4 scaling, in this case 1. The van der Waals interactions are modified by using the special 1–4 parameters defined in the parameter files. Local interaction distance common to both electrostatic and van der Waals calculations was set to 12 Å. A smooth switching function was applied to distances larger than 10 Å and the distance between pairs for inclusion in pair lists was set to 14 Å. Electrostatic interactions

[1] N. L. Allinger, Y. H. Yuh and J. H. Lii, *J. Am. Chem. Soc.* **1989**, *111*, 8551-8566.
[2] J. W. Ponder, *TINKER Version 7.1*, **2015**, http://dasher.wustl.edu/tinker
[3] J. C. Phillips, R. Braun, W. Wang, J. Gumbart, E. Tajkhorshid, E. Villa, C. Chipot, R. D. Skeel, L. Kalé and K. Schulten, *J. Comput. Chem.* **2005**, *26*, 1781-1802.
[4] S. E. Feller, Y. Zhang, R. W. Pastor and B. R. Brooks, *J. Chem. Phys.* **1995**, *103*, 4613-4621.

were computed via the particle-mesh Ewald algorithm,[5] with a mesh spacing of < 0.12 nm. All chemical components of the simulations were represented in all-atom detail by CGenFF version 3.0.1.[6] The chloroform parameters were based on the original DH model from Dietz and Heinzinger,[7] and translated into CHARMM format in Ref 8. The parameterization of organic guests **1**, **2** and fullerene were assigned using the ParamChem web interface (CGenFF program version 1.0.0).[9]

First, a cubic box of chloroform was created by using the PackMol package[10] with dimensions 60 × 60 × 60 Å^3. The initial solvent box contained 1624 molecules (8120 atoms) to match the density of chloroform (1.49 g/cm^3). The solvent box was minimized and equilibrated during a 1.25 ns NPT simulation (T = 298 K and P = 1 atm). A very small variation in the density of the simulated box from 1.49 to 1.47 g/cm^3 confirmed the reliability of the force-field. Then, a graphene sheet of 1002 atoms was soaked into the solvent box along with the desired organic molecule target of the interaction (monopodal **1**, tripodal **2** or fullerene). The boundary threshold in the solute–solvent interaction was set to 2.4 Å. Long molecular dynamics simulations were carried out for the composite boxes under the NPT ensemble (T = 298 K and P = 1 atm), with a time step of 2 fs. Covalent bonds involving hydrogen atoms were constrained using the rigidBonds keyword. Simulations of 8×10^7 and 20×10^7 steps (simulation time = 160 and 400 ns) were calculated for fullerene and monopod **1**, respectively. In tripod **2**, dynamics of 40×10^7 steps (simulation time = 800 ns) were performed for two initial conformations, with the C_{60} ball either interacting or not with the graphene sheet. Note that the coordinates of graphene atoms were frozen along the MM/MD simulations for simplicity.

Figure S18 displays the evolution of the conformations adopted by monopodal **1** along its non-covalent interaction with graphene. During the NPT simulation, guest **1** predominantly lies in a folded conformation characterized by a small centroid–centroid C_{60}–pyrene

[5] T. Darden, D. York and L. Pedersen, *J. Chem. Phys.* **1993**, *98*, 10089-10092.
[6] K. Vanommeslaeghe, E. Hatcher, C. Acharya, S. Kundu, S. Zhong, J. Shim, E. Darian, O. Guvench, P. Lopes, I. Vorobyov and A. D. MacKerell, *J. Comput. Chem.* **2010**, *31*, 671-690.
[7] W. Dietz and K. Heinzinger, *Ber. Bunsen-Ges. Phys. Chem* **1985**, *89*, 968-977.
[8] W. Yu, X. He, K. Vanommeslaeghe and A. D. MacKerell, *J. Comput. Chem.* **2012**, *33*, 2451-2468.
[9] (a) K. Vanommeslaeghe and A. D. MacKerell, *J. Chem. Inf. Model.* **2012**, *52*, 3144-3154; (b) K. Vanommeslaeghe, E. P. Raman and A. D. MacKerell, *J. Chem. Inf. Model.* **2012**, *52*, 3155-3168.
[10] L. Martínez, R. Andrade, E. G. Birgin and J. M. Martínez, *J. Comput. Chem.* **2009**, *30*, 2157-2164.

distance of around 9 Å. However, at some points of the dynamics (0–20 ns and ca. 230 ns in Figure S18b), monopodal **1** adopts an extended arrangement characterized by a long C_{60}–pyrene distance of 14–18 Å. Moreover, the fullerene ball interacts with the graphene sheet along the whole simulation with short intermolecular contacts calculated at 2.9–3.1 Å and a distance between the centroid of C_{60} and the graphene plane around 6–7 Å (Figure S18c). These results are fully in accord with those obtained in the gas-phase simulations (Figure S15).

Moving to derivative **2**, long dynamics of 800 ns were carried out starting from two different initial dispositions of tripod **2** either interacting with graphene through the three pyrene units and the fullerene head (Figure S19), which corresponds to the most stable conformation found in gas phase (Figure 16e), or only through the pyrene feet with the C_{60} in axial position (Figure S21). In the first dynamics, the conformation of tripod **2** with a clear C_{60}–graphene interaction calculated around 2.9–3.1 Å remains over time up to 525 ns (regime 1 in Figure 19). Thereafter, solvent molecules enter between C_{60} and graphene, and the fullerene head moves away to acquire more extended (axial) dispositions (regime 2). Representative snapshots of each regime are depicted in Figure S20. Figure S19c indicates the amplitude of the conformations explored in **2** along the dynamics for the two regimes. Regime 1 is characterized by a range of tilting angle θ values between 95 and 120º, due to the favorable interaction between the C_{60} ball and the graphene surface. Otherwise, a wider range of θ values (130–175º) is calculated in regime 2 due to the freedom of C_{60} to move when soaked into the solvent.

Starting from a tripodal **2** with the fullerene head positioned apical to the graphene sheet, NPT simulations along 800 ns predict that this conformation persists over time (regime 2), and the C_{60} does not reach graphene for interaction (Figure S21). These results indicate that the conformations in which the fullerene C_{60} is positioned apical (regime 2) predominate in solution compared to the folded structures in which C_{60} interacts with graphene (regime 1).

Finally, a control dynamics was undertaken for the interaction between pristine C_{60} and graphene along 160 ns. MM/MD simulations (Figure S22) starting from a C_{60} interacting with graphene (short C_{60}–graphene contacts calculated at 2.9-3.1 Å) show that this conformation lasts over time up to ca. 110 ns. Then, the C_{60}–graphene interaction breaks

apart due to the inclusion of solvent molecules in between, and the fullerene ball moves away to be soaked into de solvent environment. These results confirm that the interaction between fullerene and graphene is not strong enough to allow stable supramolecular nanobuds in solution.

4. Synthetic details, characterization and collection of spectra

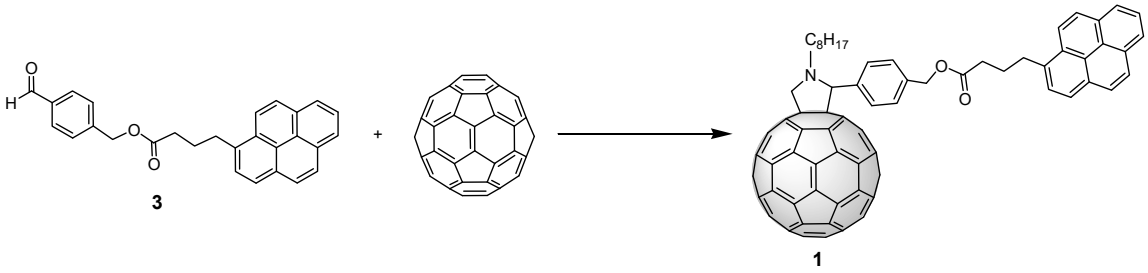

Scheme 1. Synthesis of the C_{60} derivative endowed with mono-pyrene units (**1**).

Synthesis of 4-formylbenzyl 4-(pyren-1-yl)butanoate (3)

A solution of 4-hydroxymethylbenzaldehyde (0.43 g, 3.15 mmol) and 4-(1-pyrenyl)butyric acid (1.36 g, 4.73 mmol) in dichloromethane (DCM) and at 0 ºC was stirred for 10 minutes under Ar atmosphere. Then 1,3-dicyclohexylcarbodiimide (DCC) (0.98 g, 4.73 mmol) and 4-(dimethylamino)pyridine (DMAP) (0.054 g, 0.44 mmol) in 10 mL of DCM were added and the mixture was stirred for another 15 minutes at 0 ºC. The cooling bath was then removed, and the solution was allowed to react at room temperature 24 hours. The reaction mixture was washed with water. The organic layer was dried with Na_2SO_4 and the solvent was removed under reduced pressure. The residue was purified by silica gel column chromatography using a DCM/hexane (8/3) mixture as eluent. The product was isolated as a yellow solid (86%).

^{1}H-NMR (300 MHz, $CDCl_3$) δ: 9.94 (s, 1H), 8.24 (d, 1H, *J* = 9.3 Hz), 8.19–7.95 (m, 7H), 7.82 (d, 1H, *J* = 7.8 Hz), 7.76 (d, 2H, *J* = 8.1 Hz), 7.38 (d, 2H, *J* = 8.1 Hz), 5.12 (s, 2H), 3.42–3.33 (m, 2H), 2.54 (t, 2H, *J* = 7.3 Hz), 2.30–2.18 (m, 2H); ^{13}C-NMR (75 MHz, $CDCl_3$) δ: 191.8, 173.1, 142.6, 135.9, 135.5, 131.4, 130.9, 130.0, 129.9, 128.8, 128.1,

127.5, 127.5, 127.4, 126.8, 125.9, 125.1, 125.0, 124.9, 124.8, 124.8, 123.3, 65.3, 33.8, 32.7, 26.7; FT-IR ($CHCl_3$), ν (cm^{-1}): 2925, 2854, 1731, 1692, 1609, 1579, 1509, 1489, 1456, 1434, 1417, 1380, 1305, 1245, 1208, 1182, 1159, 1142, 1100, 1065, 1033, 1007, 972, 909, 843, 818, 781, 760, 721, 709, 682, 621, 588; UV-Vis ($CHCl_3$), λ_{max} (nm) (ε (L mol^{-1} cm^{-1})): 314 (12588), 329 (27529), 345 (32824); EI-MS (m/z) calculated for $C_{28}H_{22}O_3$ [M^+]: 406.1569 found: 406.1563.

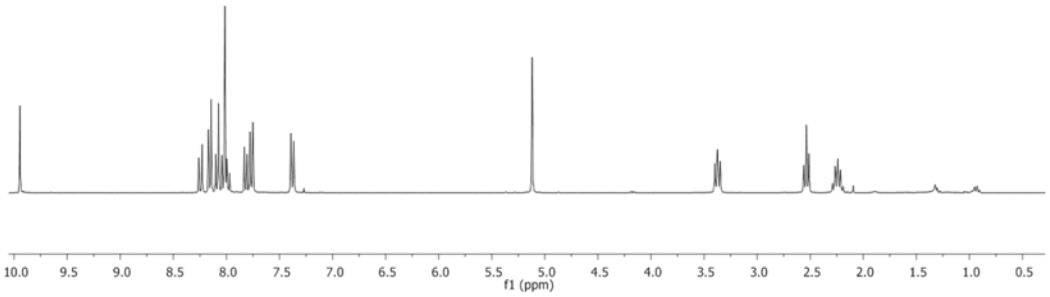

^{1}H NMR spectrum (300 MHz, $CDCl_3$) of **3**.

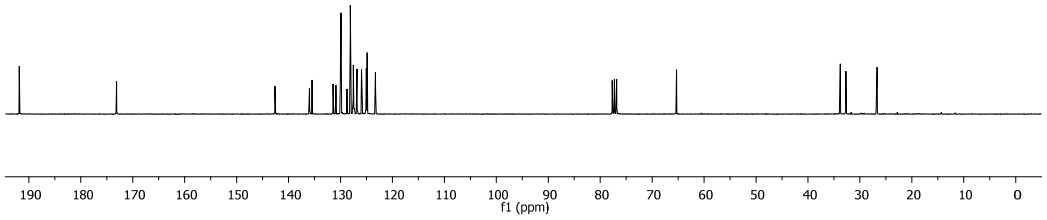

^{13}C NMR spectrum (75 MHz, $CDCl_3$) of **3**.

Synthesis of *N*-octyl-2-{4-[6-(pyren-1-yl)-2-oxa-3-oxo-hexyl]phenyl}pyrrolidino [3,4:1,2] [60]fullerene (1)

N-octylglycine (0.14 g, 0.74 mmol) and 4-formylbenzyl 4-(pyren-1-yl)butanoate **3** (0.07 g, 0.18 mmol) were added to a solution of C_{60} (0.20 g, 0.28 mmol) in toluene (100 mL). The resulting solution was heated overnight at reflux under Ar atmosphere. The solvent was removed under reduced pressure and the crude was purified by silica gel column chromatography using as eluent a gradient from C_2S to C_2S/toluene (1/1). The product was isolated as a brown solid (38%).

^{1}H-NMR (700 MHz, $CDCl_3$) δ: 8.22 (d, 1H, *J* = 9.2 Hz), 8.19-7.97 (m, 8H), 7.80 (d, 2H, *J* = 7.7 Hz), 7.44 (d, 2H, *J* = 7.7 Hz), 5.20 – 5.14 (m, 2H), 5.08 (d, 1H, *J* = 9.3 Hz), 5.04 (s, 1H), 4.10 (d, 1H, *J* = 9.3 Hz), 3.33 – 3.29 (m, 2H), 3.18 (m, 1H), 2.55 – 2.49 (m, 3H), 2.23 – 2.16 (m, 2H), 1.99 – 1.91 (m, 1H), 1.88 – 1.79 (m, 1H), 1.50 – 1.28 (m, 10H), 0.91 (t, 3H, *J* = 7.0 Hz); ^{13}C-NMR (175 MHz, $CDCl_3$) δ: 173.3, 156.5, 154.2, 153.4, 153.3, 147.3, 146.6, 146.4, 146.3, 146.2, 146.1, 146.0, 145.8, 145.6, 145.5, 145.4, 145.3, 145.2, 145.1, 144.7, 144.4, 144.3, 143.0, 142.9, 142.6, 142.5, 142.4, 142.3, 142.2, 142.1, 142.0, 141.8, 141.6, 141.3, 140.1, 139.8, 139.3, 137.6, 136.8, 136.5, 136.2, 135.8, 135.6, 131.4, 130.9, 130.0, 128.8, 127.5, 127.4, 126.8, 125.9, 125.1, 125.0, 124.8, 123.3, 82.3, 76.6, 68.9, 66.9, 65.9, 53.2, 34.0, 32.7, 32.0, 29.7, 29.3, 28.4, 27.5, 26.9, 22.7, 14.2; FT-IR (KBr), ν (cm^{-1}): 2923, 2852, 2796, 1736, 1605, 1511, 1460, 1426, 1379, 1301, 1238, 1182, 1025, 967, 843, 714, 576, 553, 527; UV-Vis (NMP), λ_{max} (nm) (ε (L mol^{-1} cm^{-1})): 313 (30667), 329 (30000), 344 (27667), 432 (3333); MALDI-TOF-MS (m/z) calculated for $C_{97}H_{41}NO_2$ [M+]: 1252.3171 found: 1252.3163.

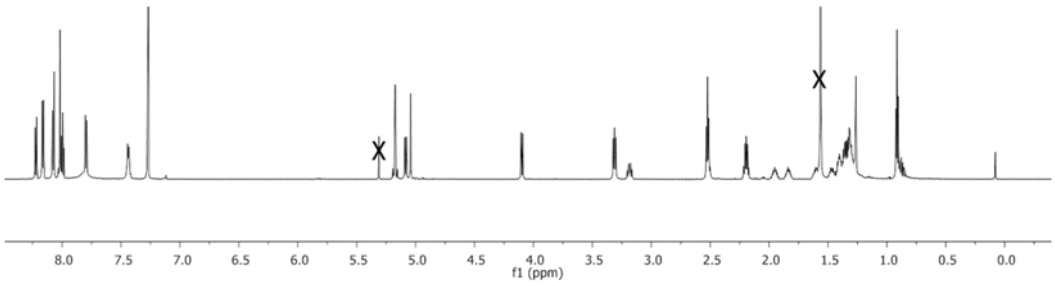

^{1}H NMR spectrum (700 MHz, $CDCl_3$) of **1**. (Traces of solvent are denoted with an X).

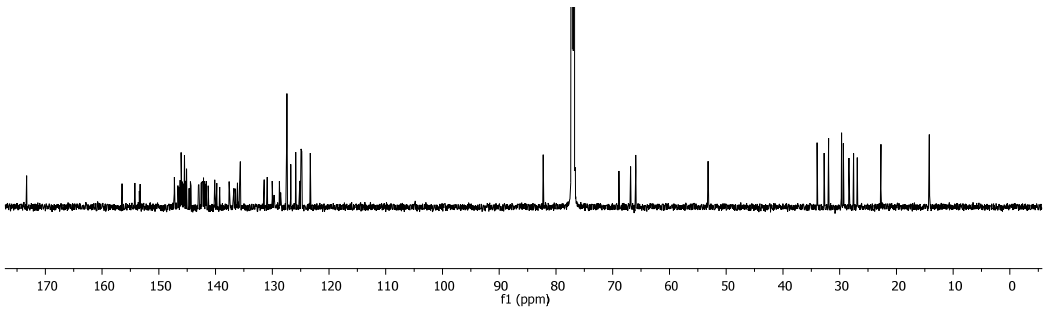

^{13}C NMR spectrum (175 MHz, $CDCl_3$) of **1**.

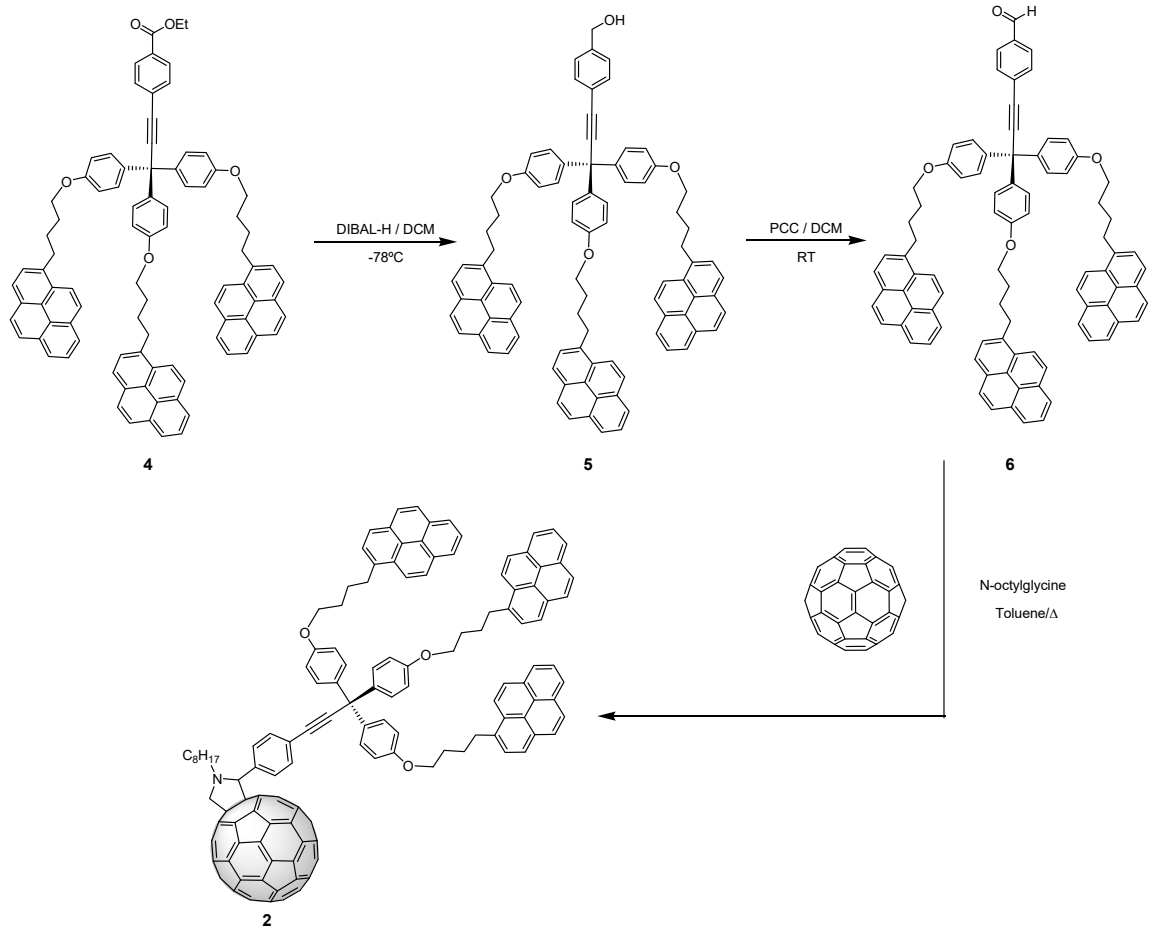

Scheme 2. Synthesis of the C_{60} derivative endowed with tripodal pyrene units (**2**).

Synthesis of ethyl 4-{3,3,3-tris[4-(4-(pyren-1-yl)butoxy)phenyl]-1-propynyl}benzoate (4)

A solution of ethyl 4-[3,3,3-tris(4-methoxyphenyl)-1-propynyl]benzoate[11] (0.09 g, 0.20 mmol), K_2CO_3 (0.25 g, 1.85 mmol) and 18-crown-6 (0.05 g, 0.18 mmol) in acetone was degassed under Ar and heated at reflux during 1 hour. After this time, 4-(1-pyrenyl)-1-butanol tosylate[12] (0.31 g, 0.72 mmol) was added in 5 mL of acetone drop by drop. The reaction was allowed to react under these conditions 3 days. The solvent was removed under reduced pressure and the solid was purified by silica gel column chromatography

[11] A. Mann, T. Alava, H. G. Craighead and W. R. Dichtel, *Angew. Chem. Int. Ed.*, 2013, **52**, 3177.
[12] J. A. Mann, J. Rodríguez-López, H. D. Abruña and W. R. Dichtel, *J. Am. Chem. Soc.,* 2011, **133**, 17614.

using a hexane/AcOEt (4/1) mixture as eluent. The product was isolated as a white solid (38%).

^{1}H-NMR (500 MHz, $CDCl_3$) δ: 8.28 (d, 3H, *J* = 9.2 Hz), 8.18-7.95 (m, 23H), 7.88 (d, 3H, *J* = 7.8 Hz), 7.54 (m, 2H), 7.19 (d, 6H, *J* = 8.8 Hz), 6.83 (d, 6H, *J* = 8.8 Hz), 4.38 (q, 2H, *J* = 7.2 Hz), 4.02 (t, 6H, *J* = 6.2 Hz), 3.42 (t, 6H, *J* = 7.6 Hz), 2.05 (m, 6H), 1.97 (m, 6H), 1.40 (t, 3H, *J* = 7.2 Hz); ^{13}C-NMR (125 MHz, $CDCl_3$) δ: 167.0, 158.3, 138.0, 137.0, 131.9, 131.8, 131.3, 130.5, 130.2, 129.8, 129.7, 129.6, 129.1, 128.9, 127.9, 127.7, 127.0, 126.2, 125.5, 125.4, 125.3, 125.2, 125.1, 123.8, 114.3, 100.0, 84.3, 68.1, 61.5, 54.6, 52.6, 33.6, 30.1, 29.7, 28.7, 14.7;]FT-IR ($CHCl_3$), ν (cm^{-1}): 2930, 2863, 1718, 1604, 1503, 1466, 1438, 1395, 1242, 1175, 1106, 1020, 961, 900, 838, 764, 729, 612; UV-Vis ($CHCl_3$), λ_{max} (nm) (ε (L mol^{-1} cm^{-1})): 314 (38732), 329 (87324), 345 (119366); MALDI-TOF-MS (m/z) calculated for $C_{90}H_{72}O_5$ [M+]: 1232.5380, found: 1232.5490.

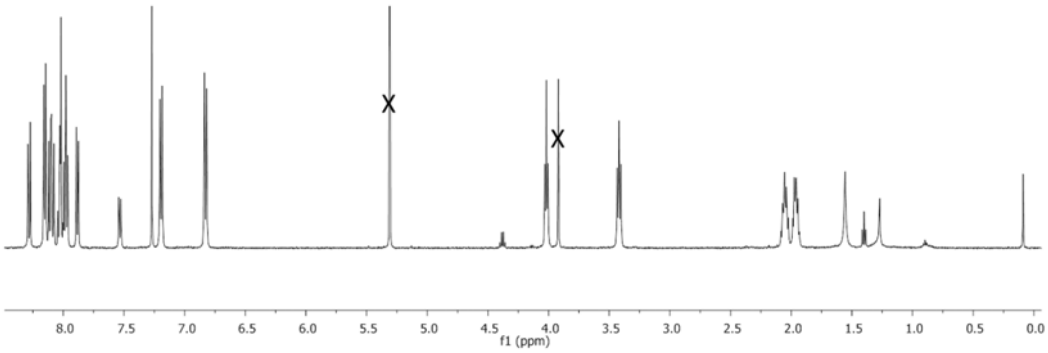

^{1}H NMR spectrum (500 MHz, $CDCl_3$) of **4**. (Traces of solvent are denoted with an X).

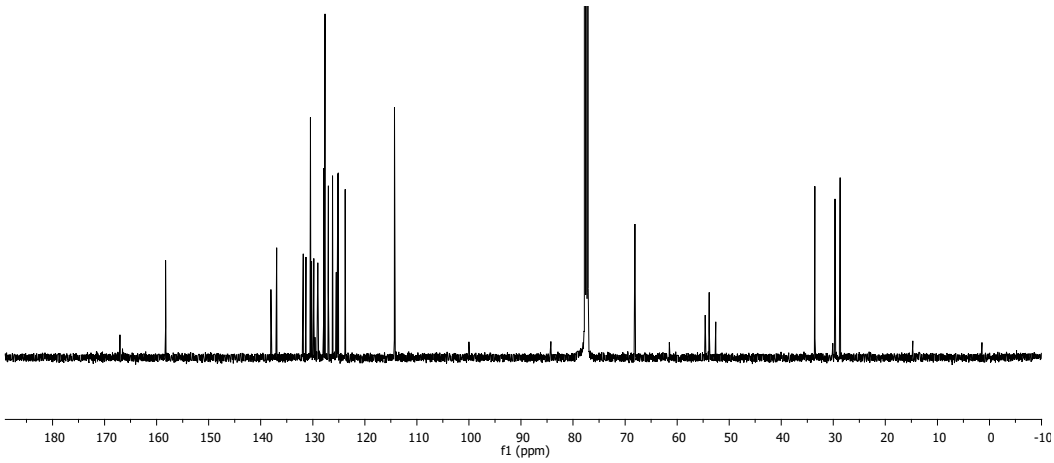

^{13}C NMR spectrum (125 MHz, $CDCl_3$) of **4.**

Synthesis of 4-{3,3,3-tris[4-(4-(pyren-1-yl)butoxy)phenyl]-1-propynyl}benzylic alcohol (5)

To a solution of ester **4** (0.08 g, 0.06 mmol) in dry DCM at –78 ºC and under Ar, was added DIBAL-H (0.07 mL, 0.07mmol) drop by drop. After 2 hours, MeOH (0.5 mL) was added to the reaction mixture and then was extracted with ether and HCl (1M), the solvent was removed under reduced pressure and the crude was purified by silica gel column chromatography using a hexane/AcOEt (1/1) mixture as eluent. The product was isolated as a white solid (58%).

^{1}H-NMR (500 MHz, $CDCl_3$) δ: 8.28 (d, 3H, *J* = 9.2 Hz), 8.18-7.95 (m, 21H), 7.88 (d, 3H, *J* = 7.8 Hz), 7.50 (d, 2H, *J* = 8.1 Hz), 7.30 (d, 2H, *J* = 8.1 Hz), 7.24 (d, 6H, *J* = 8.8 Hz), 6.84 (d, 6H, *J* = 8.8 Hz), 4.68 (s, 2H), 4.01 (t, 6H, *J* = 6.2 Hz), 3.41 (t, 6H, *J* = 7.6 Hz), 2.10 – 2.00 (m, 6H), 1.99 – 1.91 (m, 6H); ^{13}C-NMR (125 MHz, $CDCl_3$) δ: 158.2, 141.0, 138.4, 137.0, 132.2, 131.9, 131.3, 130.5, 130.3, 129.1, 127.9, 127.7, 127.1, 127.0, 126.2, 125.5, 125.4, 125.3, 125.2, 125.1, 123.8, 123.5, 114.3, 96.8, 84.7, 68.1, 65.4, 54.5, 33.6, 29.7, 28.7; FT-IR ($CHCl_3$), ν (cm^{-1}): 3455, 3040, 2931, 2864, 1604, 1502, 1466, 1388, 1295, 1241, 1175, 1108, 1036, 905, 837, 726, 644, 615; UV-Vis ($CHCl_3$), λ_{max} (nm) (ε (L mol^{-1} cm^{-1})): 314 (37698), 329 (83730), 345 (111508); MALDI-TOF-MS (m/z) calculated for $C_{88}H_{70}O_4$ [M+]: 1190.5274, found: 1190.5284.

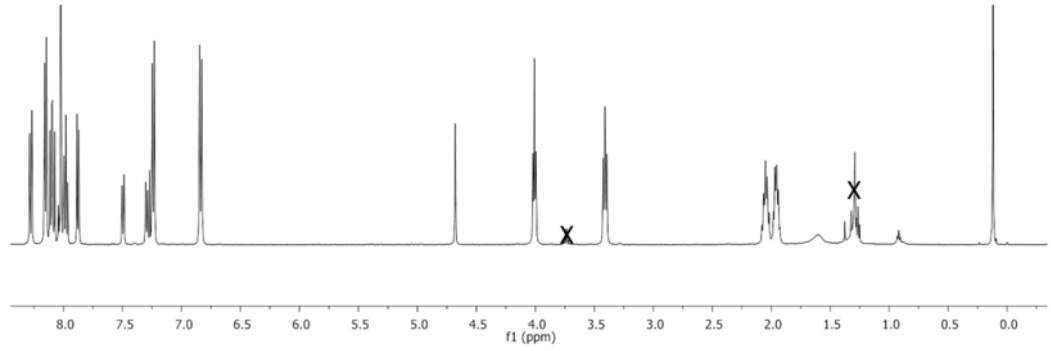

^{1}H NMR spectrum (500 MHz, $CDCl_3$) of **5**. (Traces of solvent are denoted with an X).

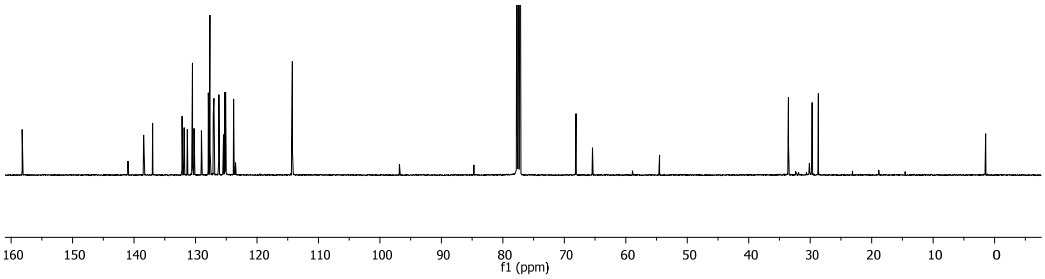

^{13}C NMR spectrum (125 MHz, $CDCl_3$) of **5**.

Synthesis of 4-{3,3,3-tris[4-(4-(pyren-1-yl)butoxy)phenyl]-1-propynyl}benzaldehyde (6)

To a solution of alcohol **5** (0.07 g, 0.06 mmol) in DCM and at room temperature, PCC (0.03 g, 0.12 mmol) was added. The mixture was allowed to react under these conditions overnight. After this time, the solvent was removed under reduced pressure and the crude was purified by silica gel column chromatography using a hexane/AcOEt (2/1) mixture as eluent. The product was isolated as a white solid (84%).

^{1}H-NMR (300 MHz, $CDCl_3$) δ: 9.99 (s, 1H), 8.28 (d, 3H, *J* = 9.3 Hz), 8.19-7.93 (m, 21H), 7.88 (d, 3H *J* = 7.8 Hz), 7.81 (d, 2H, *J* = 8.2 Hz), 7.62 (d, 2H, *J* = 8.2 Hz), 7.19 (d, 6H, *J* = 8.8 Hz), 6.83 (d, 6H, *J* = 8.8 Hz), 4.02 (t, 6H, *J* = 6.0 Hz), 3.42 (t, 6H, *J* = 7.4 Hz), 2.01 (m, 12H); ^{13}C-NMR (75 MHz, $CDCl_3$) δ: 191.5, 157.9, 137.5, 136.6, 135.2, 132.2, 131.5, 130.9, 130.1, 129.9, 129.5, 128.7, 127.5, 127.3, 126.6, 125.8, 125.1, 124.9, 124.8, 124.7, 123.4, 114.0, 100.9, 88.9, 67.7, 54.3, 33.2, 29.7, 28.3; FT-IR ($CHCl_3$), ν (cm^{-1}): 2926, 2857, 1699, 1603, 1505, 1466, 1387, 1297, 1246, 1177, 1110, 1040, 964, 902, 841, 757, 717, 618; UV-Vis ($CHCl_3$), λ_{max} (nm) (ε (L mol^{-1} cm^{-1})): 313 (28571), 329 (48485), 345 (70563); MALDI-TOF-MS (m/z) calculated for $C_{88}H_{68}O_4$ [M+]: 1188.5118, found: 1188.5156.

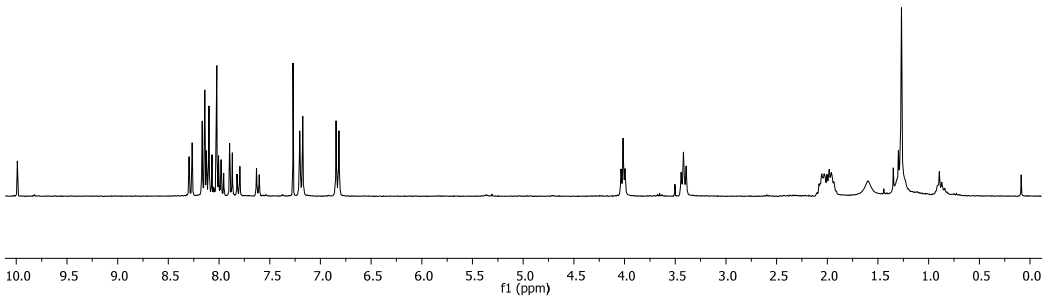

^{1}H NMR spectrum (300 MHz, $CDCl_3$) of **6**.

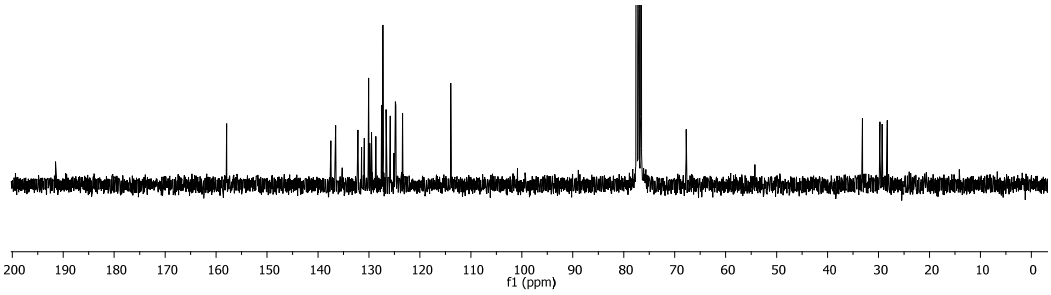

^{13}C NMR spectrum (75 MHz, $CDCl_3$) of **6**.

Synthesis of *N*-octyl-2-(4-(3,3,3-tris(4-(4-(1-pyrenyl)butoxy)phenyl)-1-propynyl)phenyl) pyrrolidino[3,4:1,2][60]fullerene (2)

N-octylglycine (0.06 g, 0.34 mmol) and **6** (0.1 g, 0.08 mmol) were added to a solution of C_{60} (0.09 g, 0.13 mmol) in toluene (100 mL). The resulting solution was heated overnight at reflux and under Ar atmosphere. The solvent was removed under reduced pressure and the crude was purified by silica gel column chromatography using as eluent a gradient from C_2S to C_2S/toluene (3/1). The product was isolated as a brown solid (35%).

^{1}H-NMR (700 MHz, $CDCl_3$) δ: 8.22 (d, 3H, *J* = 9.2 Hz), 8.17-7.91 (m, 21H), 7.82 (d, 3H, *J* = 7.7 Hz), 7.71 (s, 2H), 7.55 (s, 2H), 7.23 (d, 6H, *J* = 8.6 Hz), 6.80 (d, 6H, *J* = 8.6 Hz), 4.92 (d, 1H, *J* = 9.1 Hz), 4.83 (s, 1H), 3.92 (t, 6H, *J* = 5.9 Hz), 3.87 (d, 1H, *J* = 9.1 Hz), 3.35 (t, 6H, *J* = 7.6 Hz), 3.09 (m, 1H), 2.40 (s, 1H), 1.98 (m, 6H), 1.95 – 1.85 (m, 6H), 1.79 (d, 1H, *J* = 4.7 Hz), 1.59 (s, 1H), 1.50 – 1.25 (m, 10H), 0.94 (t, 3H, *J* = 6.8 Hz); ^{13}C-NMR (175 MHz, $CDCl_3$) δ: 157.8, 156.3, 153.9, 153.1, 147.1, 146.5, 146.2, 146.1, 146.0, 145.9, 145.8, 145.7, 145.5, 145.3, 145.1, 145.0, 144.9, 144.5, 144.4, 144.2, 142.9, 142.7, 142.5, 142.3, 142.1, 142.0, 141.9, 141.8, 141.7, 141.6, 141.4, 141.3, 139.9, 139.7, 139.5, 137.9, 137.3, 136.7, 136.6, 136.4, 135.7, 135.5, 131.9, 131.5, 130.9, 130.1, 129.9, 129.4, 128.7, 127.6, 127.3, 126.6, 125.8, 125.2, 125.1, 124.9, 124.8, 123.8, 123.4, 113.9, 97.0, 84.4, 82.2, 76.4, 68.8, 67.7, 66.7, 54.2, 53.1, 33.2, 32.1, 29.8, 29.4, 29.3, 28.4, 28.3, 27.7, 22.8, 14.3; FT-IR (KBr), ν (cm^{-1}): 2925, 2856, 1605, 1504, 1463, 1383, 1299, 1244, 1178, 1114, 1040, 840, 760, 714, 616, 585, 553, 527; UV-Vis (NMP), λ_{max} (nm) (ε (L mol^{-1} cm^{-1})): 315 (45395),

329 (53289), 345 (51974), 433 (3289); MALDI-TOF-MS (m/z) calculated for $C_{157}H_{87}NO_3$ [M+]: 2033.6686, found: 2033.6756.

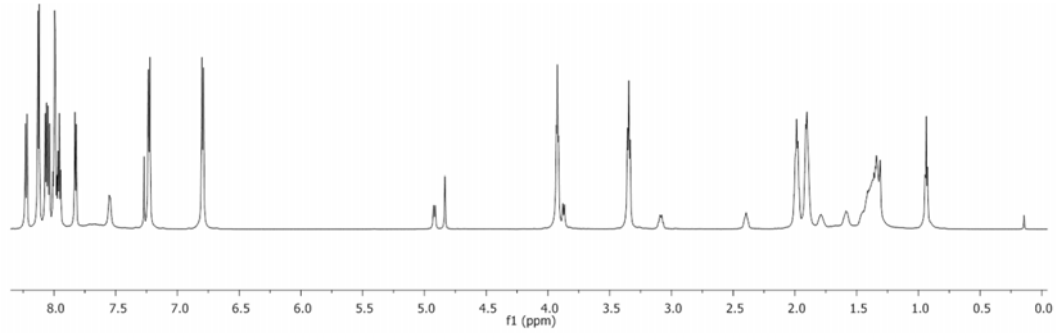

^{1}H NMR spectrum (700 MHz, $CDCl_3$) of **2**.

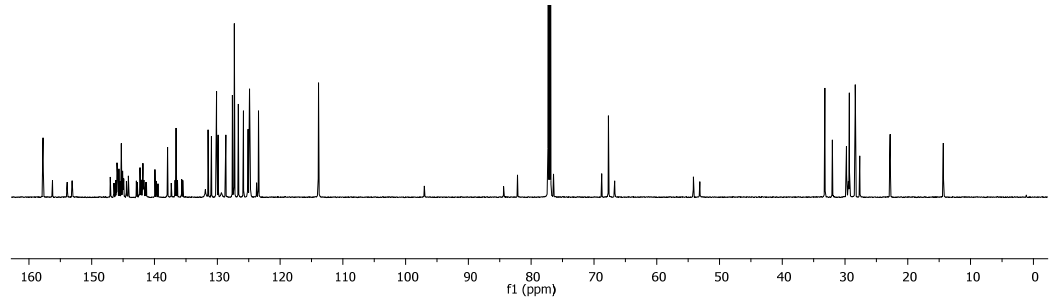

^{13}C NMR spectrum (175 MHz, $CDCl_3$) of **2**.

Synthesis of the monopodal complex (1·graphene)

A sample of 4 mg of **1** was mixed with 20 mL of the graphene dispersion previously obtained in NMP. This mixture was sonicated during 30 min. After this time, the mixture was filtered on a PTFE membrane and washed with dichloromethane until the filtrate was transparent to afford the corresponding supramolecular complex.

FT-IR (KBr), ν (cm^{-1}): 2925, 2855, 1736, 1583, 1457, 1384, 1121, 1098, 1039, 843, 721, 667, 527, 470.

TGA (N_2 atmosphere): weight loss and temperature desorption (organic groups): 8.94%, 600 ºC.

Raman: I_D/I_G = 0.10

UV-Vis (NMP), λ_{max} (nm): 327, 345.

Synthesis of the tripodal complex (2·graphene)

A sample of 7 mg of **2** was mixed with 20 mL of the FLG dispersion previously obtained in NMP. This mixture was sonicated during 30 min. After this time, the mixture was filtered on a PTFE membrane and washed with dichloromethane until the filtrate was transparent to afford the corresponding supramolecular complex.

FT-IR (KBr), ν (cm^{-1}): 2926, 2855, 1582, 1432, 1384, 1247, 1110, 1034, 841, 655, 527, 470.

TGA (N_2 atmosphere): weight loss and temperature desorption (organic groups): 17.30%, 600 ºC.

Raman: I_D/I_G = 0.08.

UV-Vis (NMP), λ_{max} (nm): 328, 345

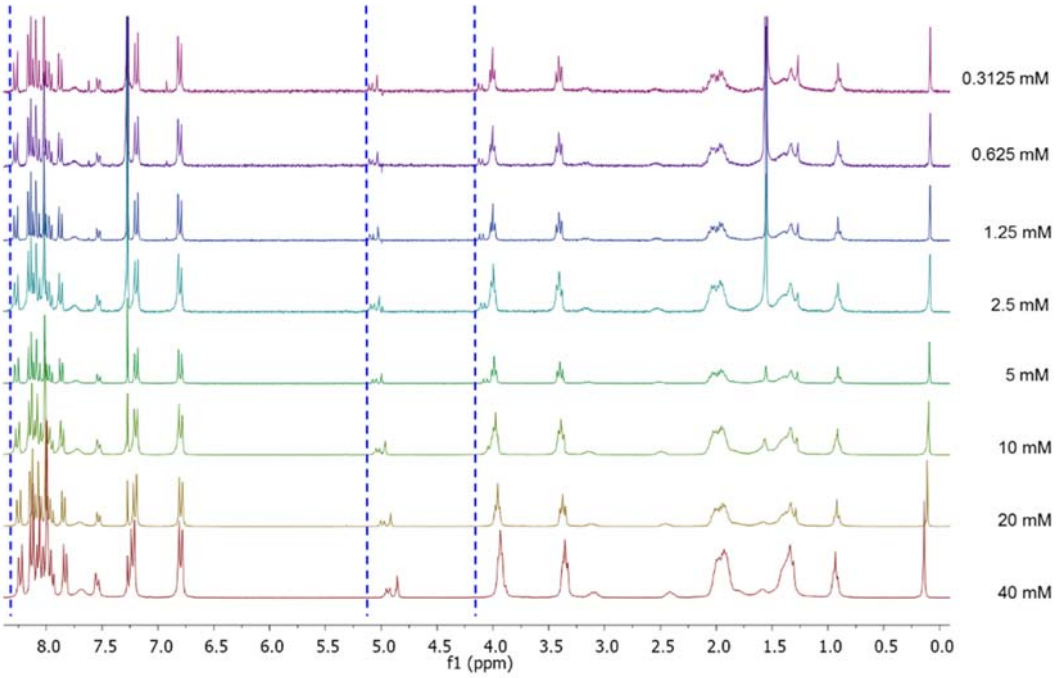

Figure S1. ^{1}H-NMR ($CDCl_3$, 300 MHz, 298 K) spectra at variable concentration for **2**.

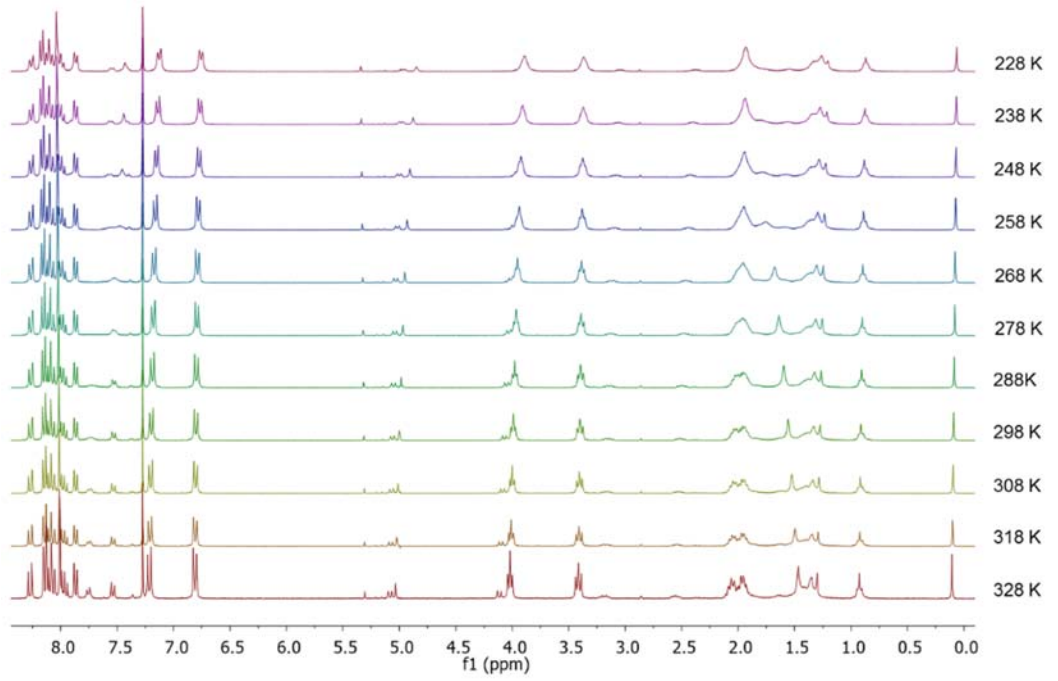

Figure S2. ^{1}H-NMR spectra ($CDCl_3$, 300 MHz) at variable temperature for **2** (5 mM).

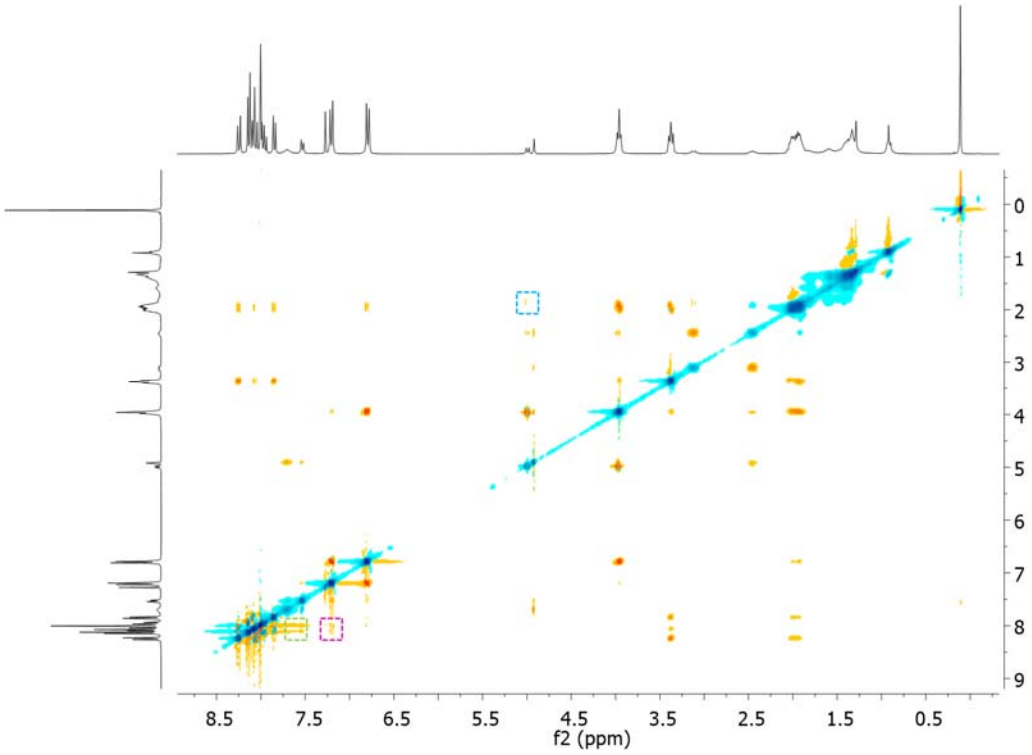

Figure S3. ROESY spectrum for **2** (20 mM).

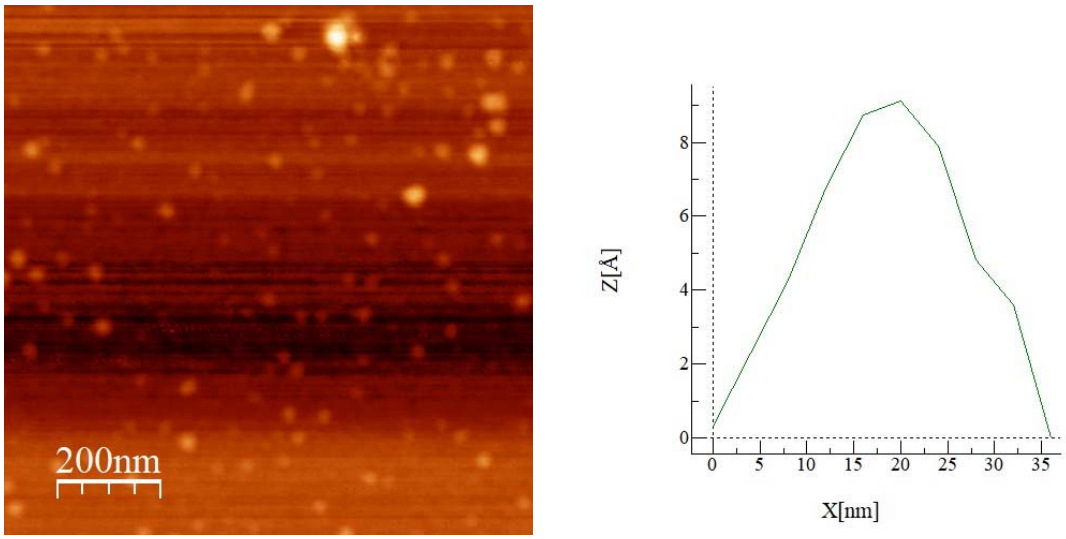

Figure S4. Tapping mode AFM image (left) and heigh profile of **1**.

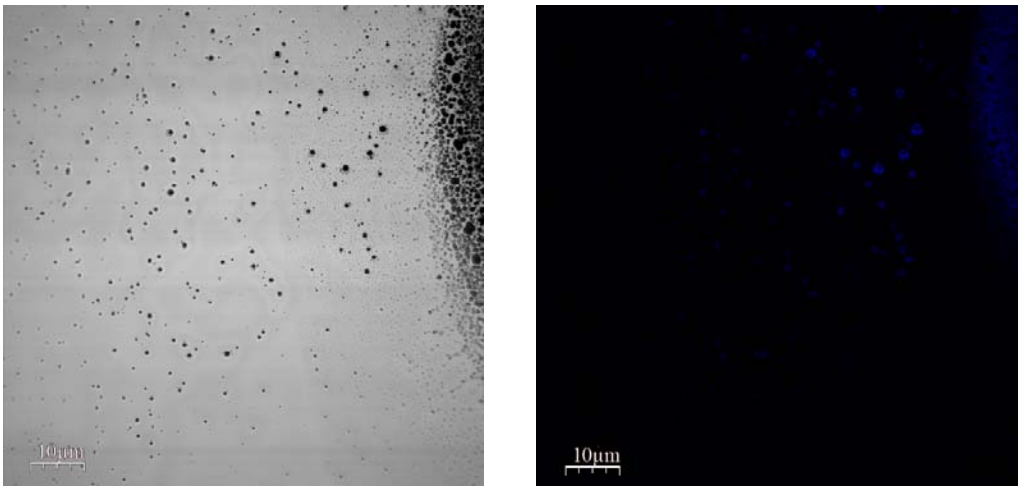

Figure S5. Confocal microscopy of a drop-cast chloroform solution of **1** with transmitted light (left) and with a λ_{exc} = 405 nm (right).

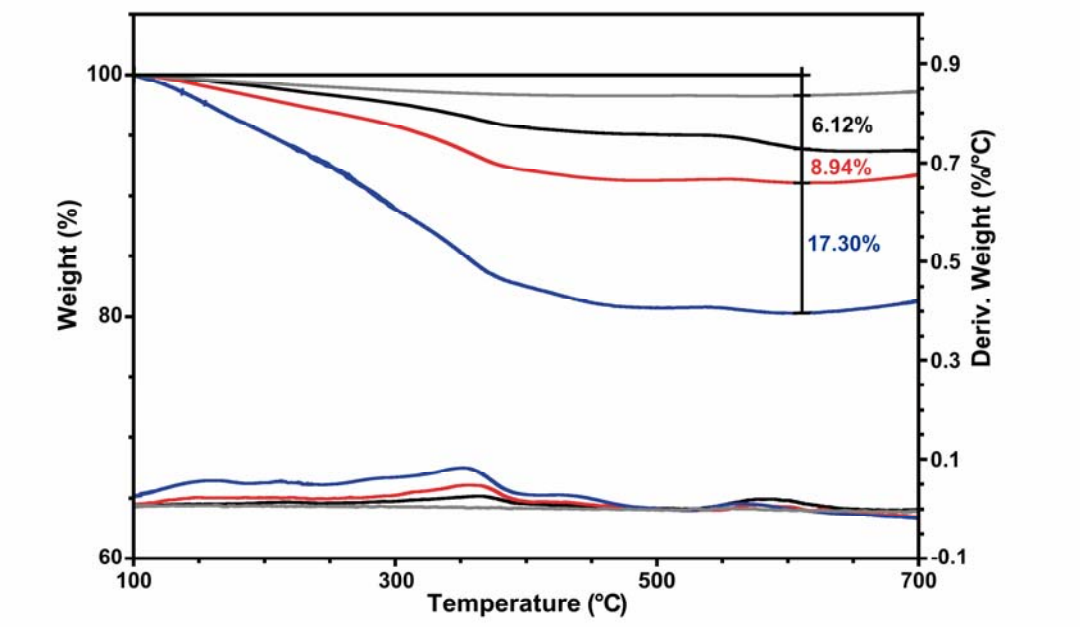

Figure S6. TGA weight loss and first derivative curves under inert conditions of graphite (grey), graphene (black), **1**·graphene complex (red) and **2**·graphene complex (blue).

(a)

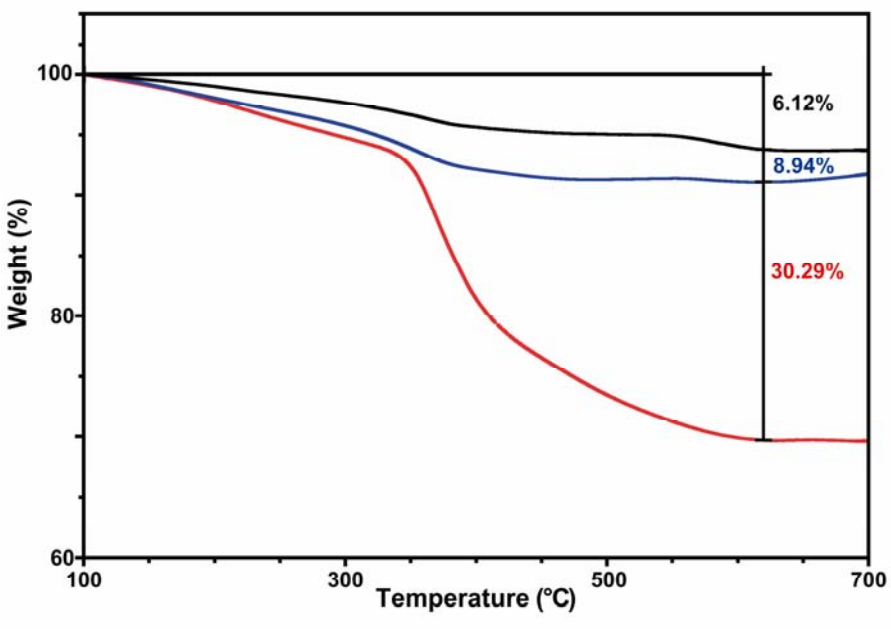

(b)

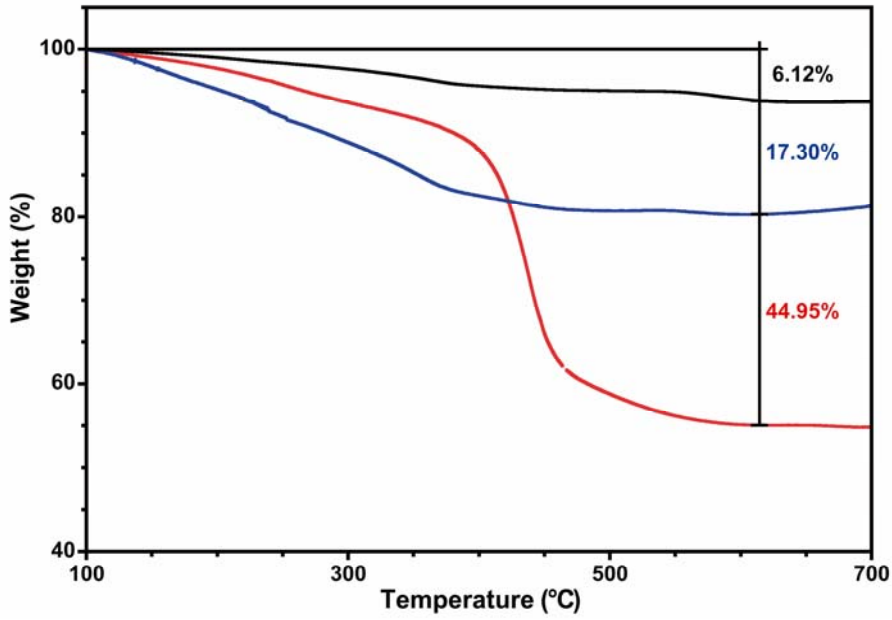

Figure S7. TGA weight loss curves under inert conditions of: (a) graphene (black), **1** (red) and **1**·graphene complex (blue). (b) graphene (black), **2** (red) and **2**·graphene complex (blue).

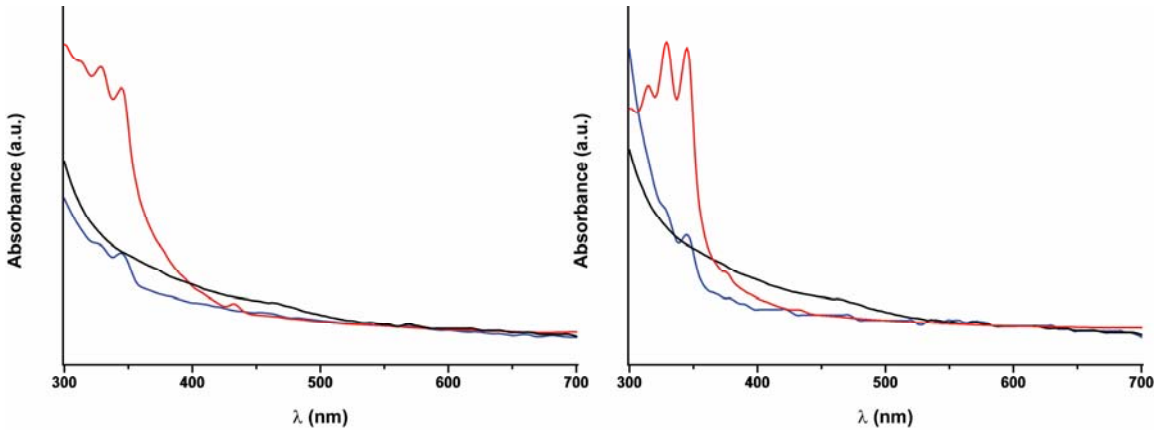

Figure S8. Left: UV-Vis spectra of graphene (black), **1** (red) and **1**·graphene complex (blue) in NMP. Right: UV-Vis spectra of graphene (black), **2** (red) and **2**·graphene complex (blue) in NMP.

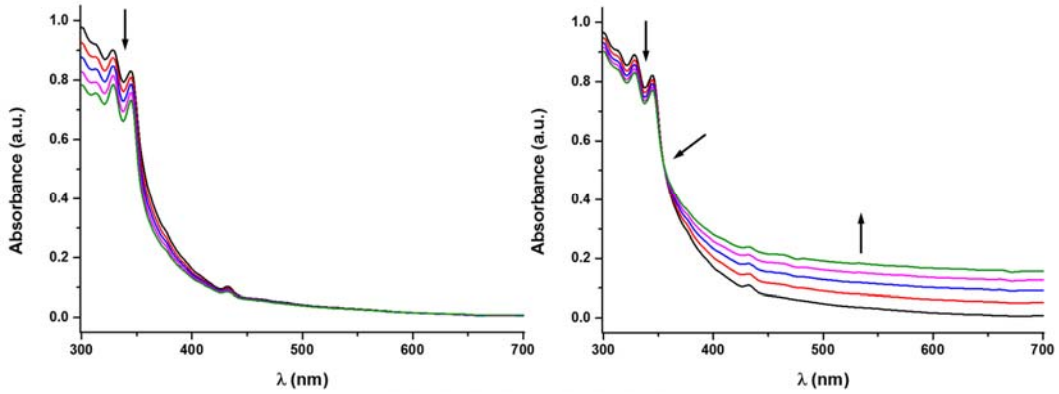

Figure S9. UV-Vis spectra obtained during the dilution (left) and titration (right) with graphene of **1** (3×10^{-5} M) in NMP. Each addition corresponds to 100 μL.

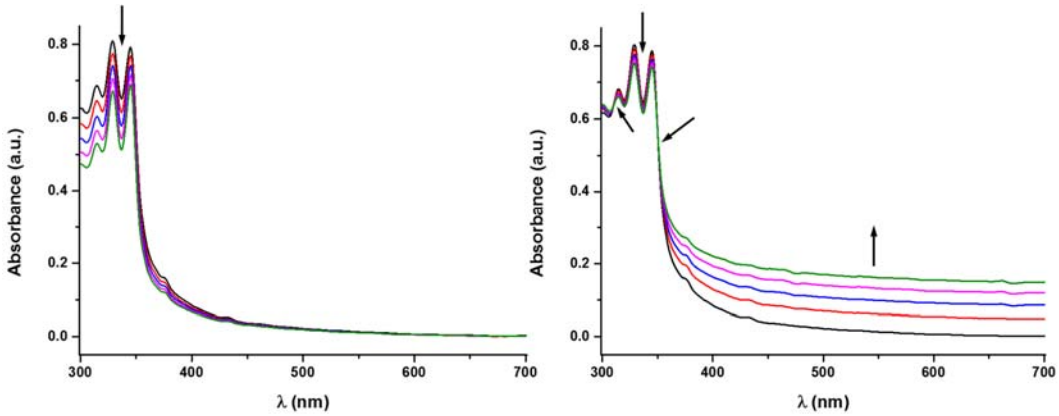

Figure S10. UV-Vis spectra obtained during the dilution (left) and titration (right) with graphene of **2** (1.52×10^{-5} M) in NMP. Each addition corresponds to 100 µL.

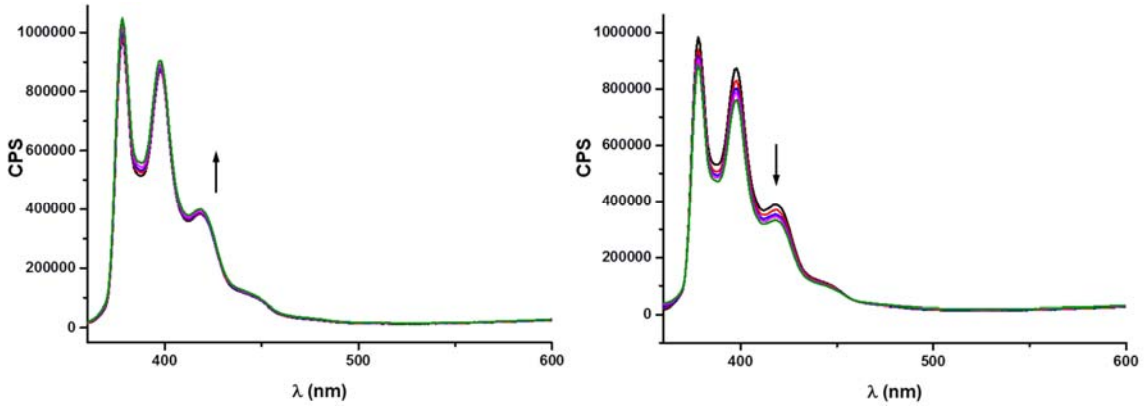

Figure S11. Fluorescence spectra obtained during the dilution (left) and titration (right) with graphene of **1** (3×10^{-5} M) in NMP. Each addition corresponds to 100 µL (λ_{exc} = 344 nm).

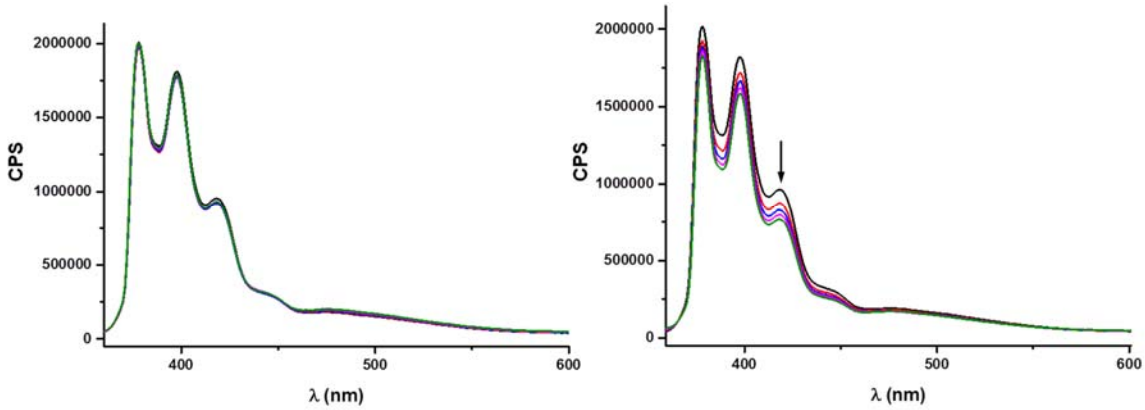

Figure S12. Fluorescence spectra obtained upon dilution (left) and titration (right) with graphene of **2** (1.52×10^{-5} M) in NMP. Each addition corresponds to 100 µL (λ_{exc} = 344 nm).

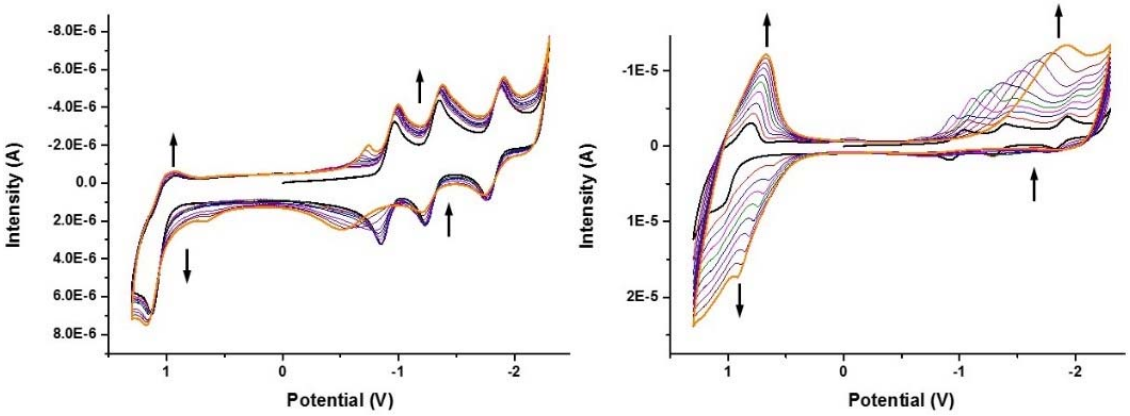

Figure S13. Consecutive cyclic voltammograms of **1** (left) and **2** (right), obtained in *o*-DCB/CH_3CN (5/1) solutions containing 0.1 M $TBAPF_6$ and using $Ag/AgNO_3$ as reference electrode, glassy carbon as working electrode and a Pt wire as counter electrode. Scan rate: 100 mV/s.

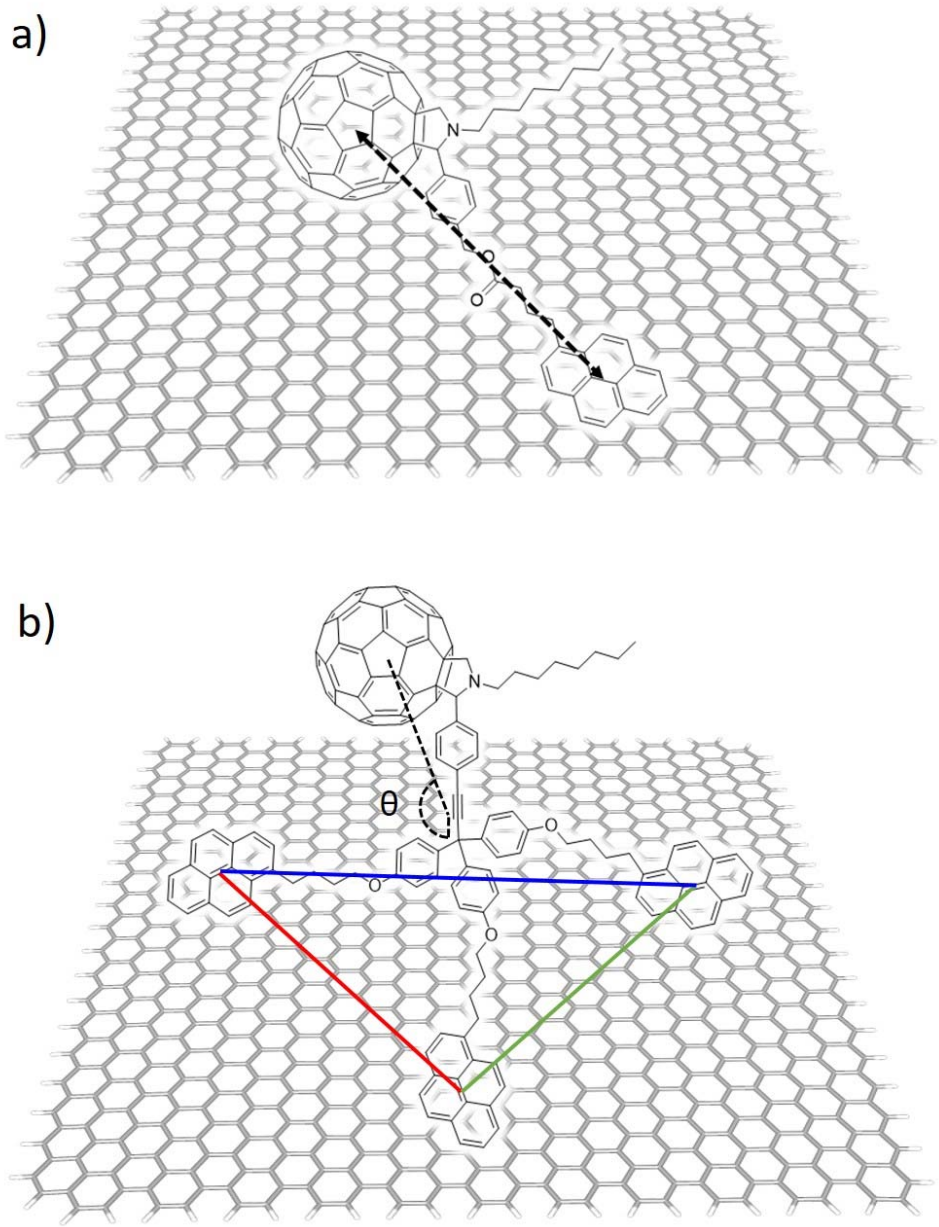

Figure S14. Intramolecular geometry parameters used to characterize the disposition of the monopodal (a) and tripodal (b) pyrene derivatives over the graphene surface along the molecular dynamics. Geometry parameters are defined as the distance between the centroids of pyrene and the C_{60} counterpart moiety for **1**, and between the centroids of the pyrene feet in **2**. The tilting angle θ is defined as the angle between the sp^3 carbon connecting the three legs, the first *sp* carbon of the triple C≡C bond and the centroid of the C_{60} head moiety.

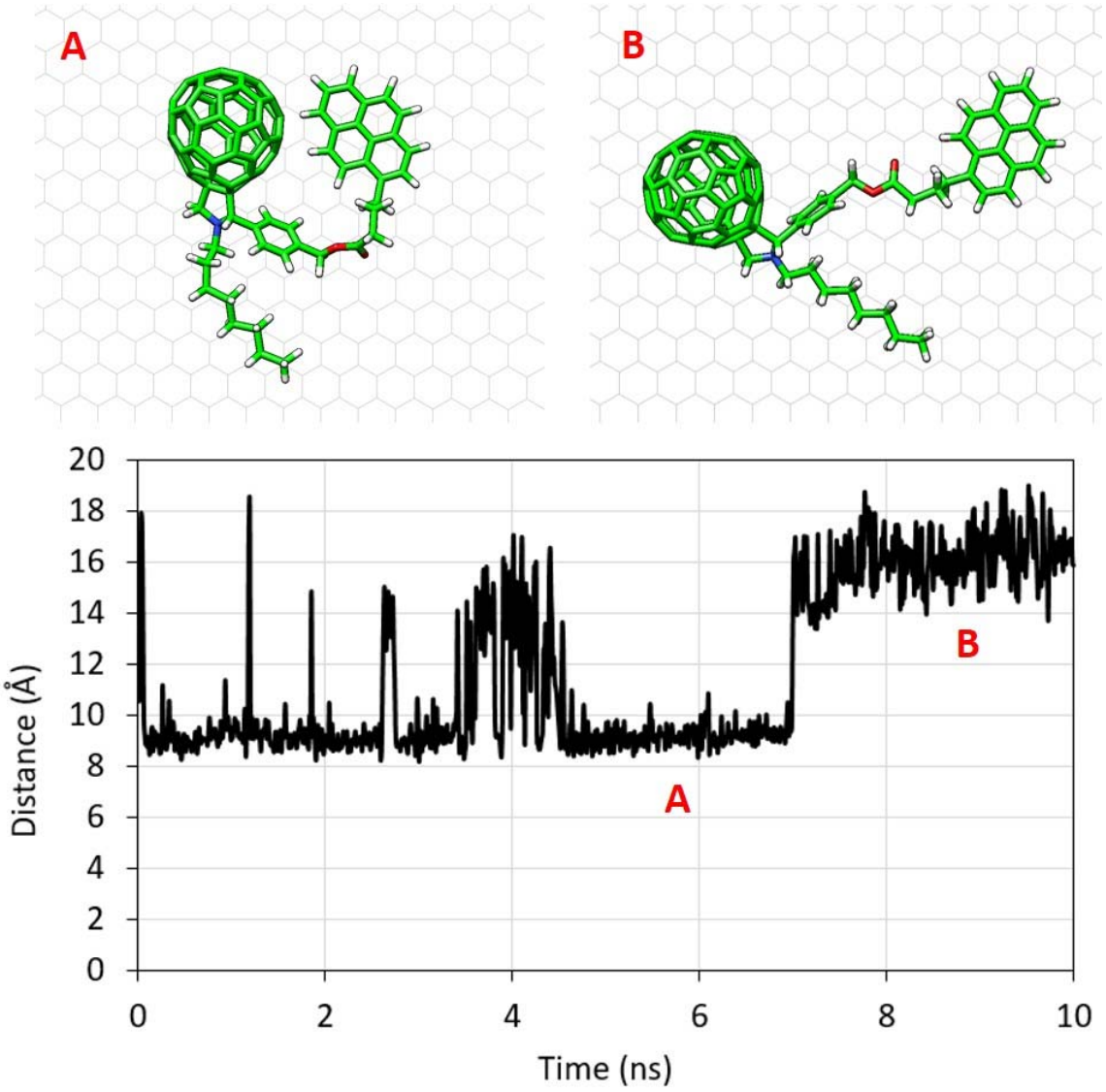

Figure S15. Evolution of the intramolecular distance between pyrene and the C_{60} counterpart (see Figure S14a) along the gas-phase molecular dynamics simulation of the supramolecular assembly of **1** with graphene. Representative snapshots of the two conformational regimes A and B are shown on the top.

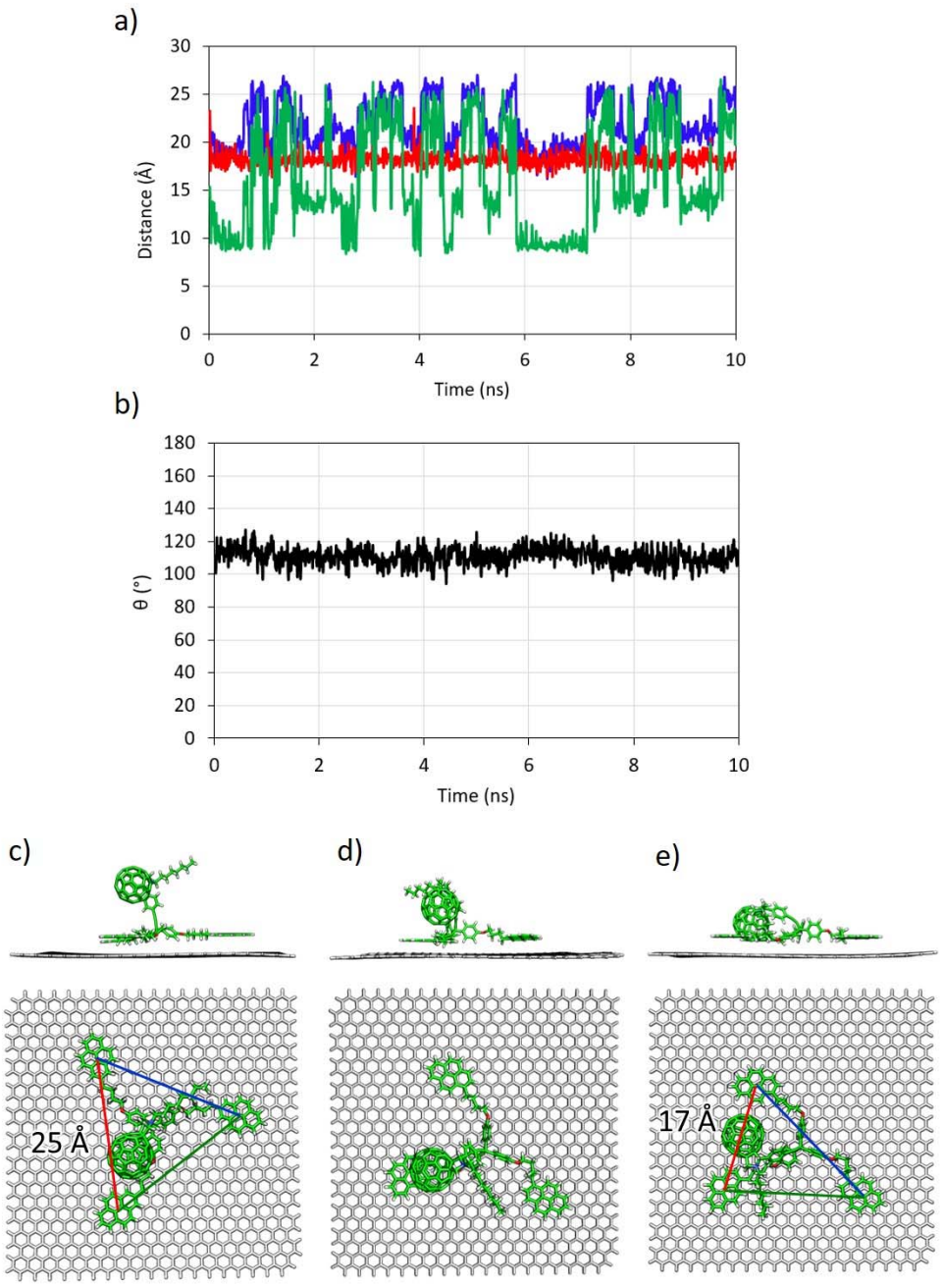

Figure S16. a) Evolution of the intramolecular distances between the three pyrene units along the gas-phase molecular dynamics simulation of the supramolecular assembly of **2** with graphene (see Figure S14b and S16c for the definition of the distances). b) Evolution of the tilting angle θ (see Figure S14b). Representative snapshots of the dynamics for **2**·graphene displaying: (c) the initial structure, (d) a fullerene–pyrene interacting conformer and (d) a fullerene–graphene interacting structure.

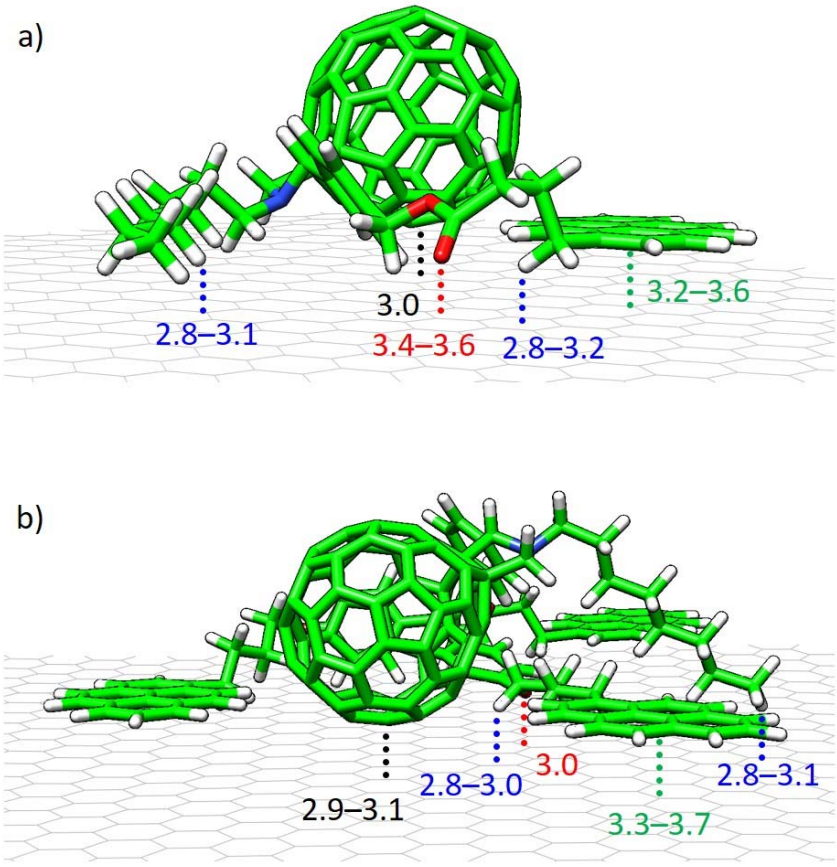

Figure S17. Representation of the different non-covalent interactions (in Å) stabilizing the supramolecular recognition of monopodal (a) and tripodal (b) nanohybrids in gas phase. Color coding: black: $C_{60}\cdots\pi$, blue: CH$\cdots\pi$, red: O$\cdots\pi$, green: π–π pyrene–graphene.

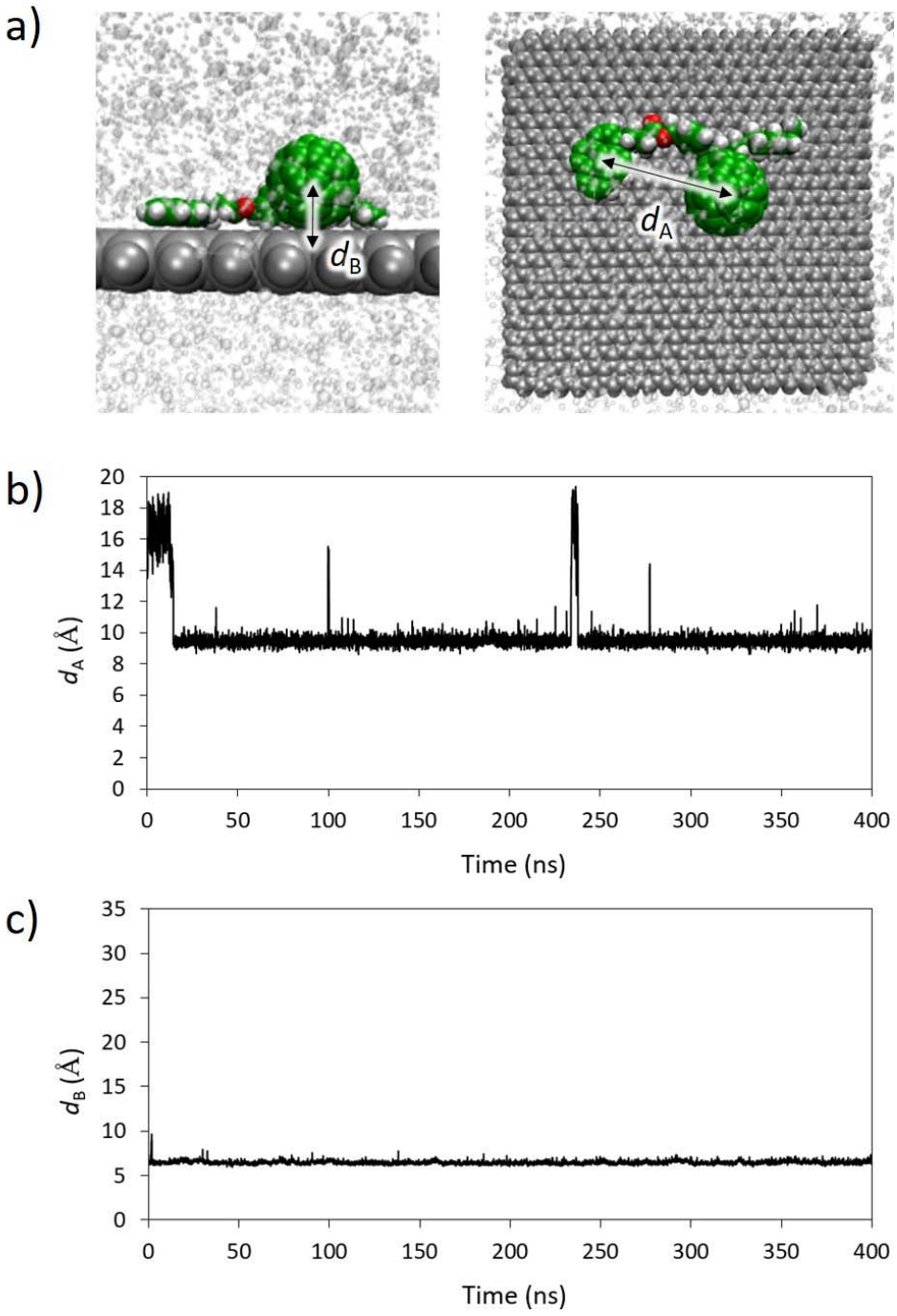

Figure S18. a) Side (left) and top (right) views of the initial structure used in the MM/MD simulation of monopodal derivative **1** interacting with graphene in the presence of the solvent. The definition of the distances between pyrene and C_{60} units (d_A), and between C_{60} and the graphene sheet plane (d_B) is included. b) and c) Evolution of the pyrene–C_{60} (d_A) and C_{60}–graphene (d_B) distances along the 400 ns simulation.

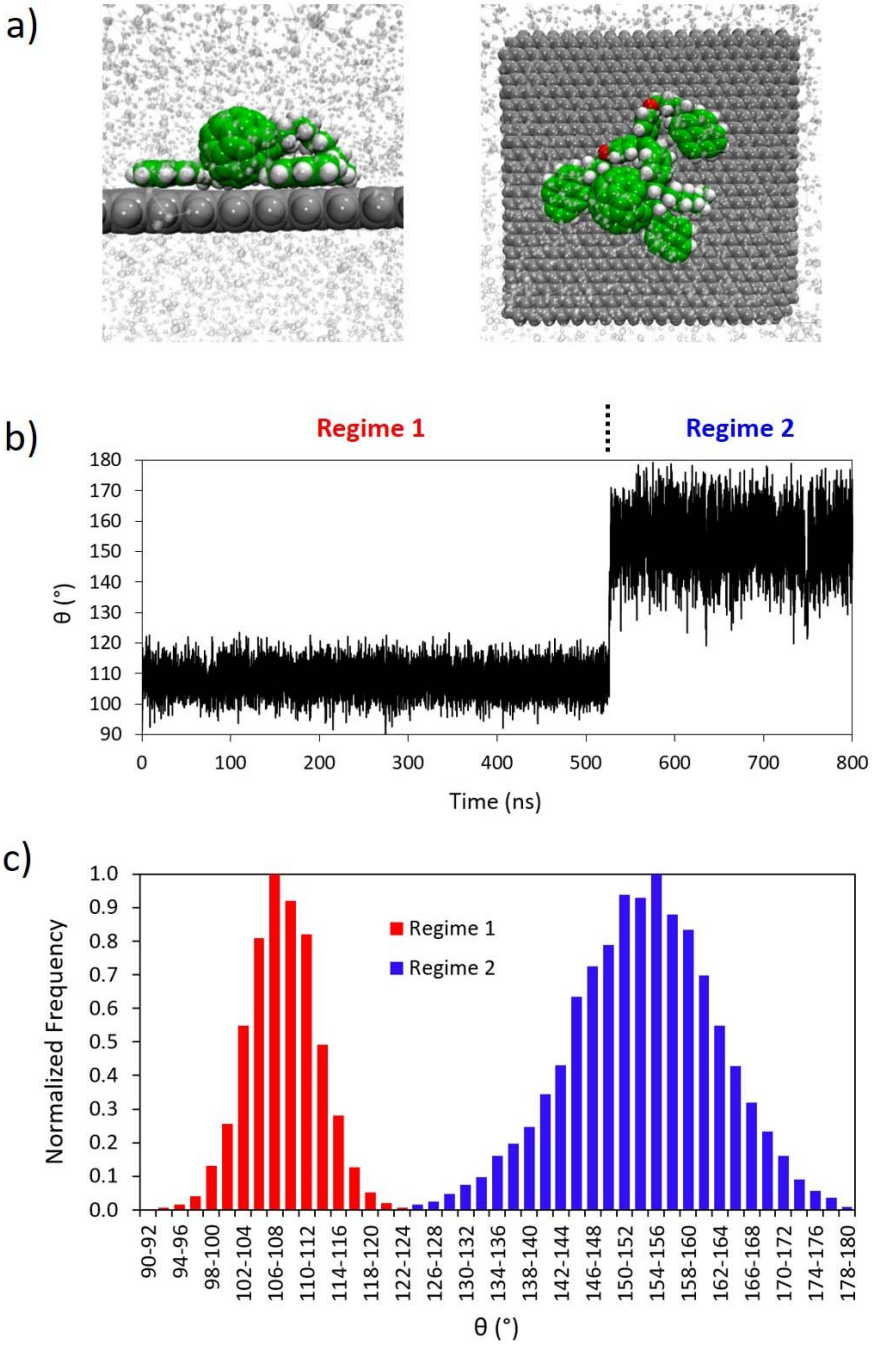

Figure S19. a) Side (left) and top (right) views of the initial structure used in the MM/MD simulation of the tripodal derivative **2** in a C_{60}–graphene interacting conformation in the presence of the solvent. b) Evolution along time of the characteristic tilting angle θ as defined in Figure S14b. c) Normalized distribution of conformations as a function of the tilting angle θ in regimes **1** (with C_{60}–graphene interaction) and **2** (without C_{60}–graphene interaction).

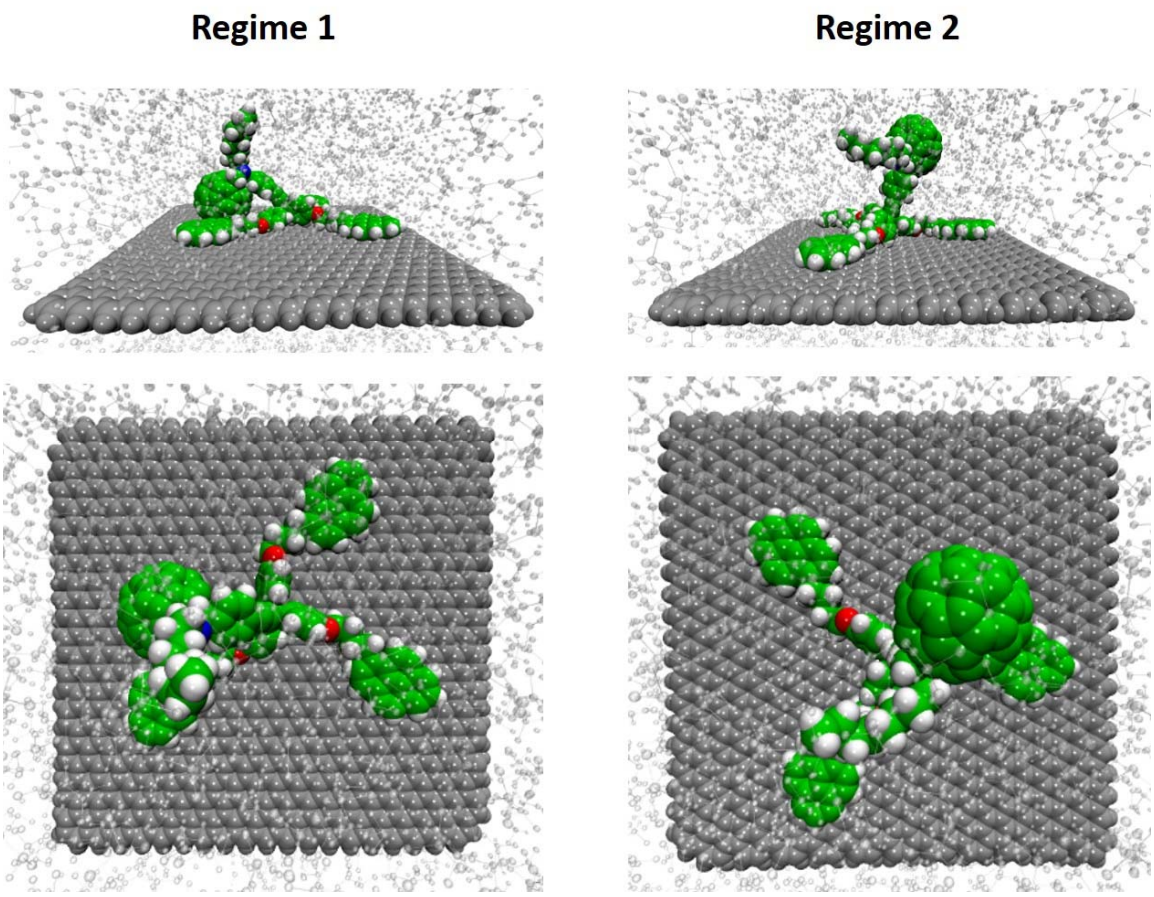

Figure S20. Representative snapshots (top – side view, and bottom – top view) of the two regimes found in the MM/MD simulation of tripodal **2**, in the presence of the solvent, starting from a C_{60}–graphene interacting conformation.

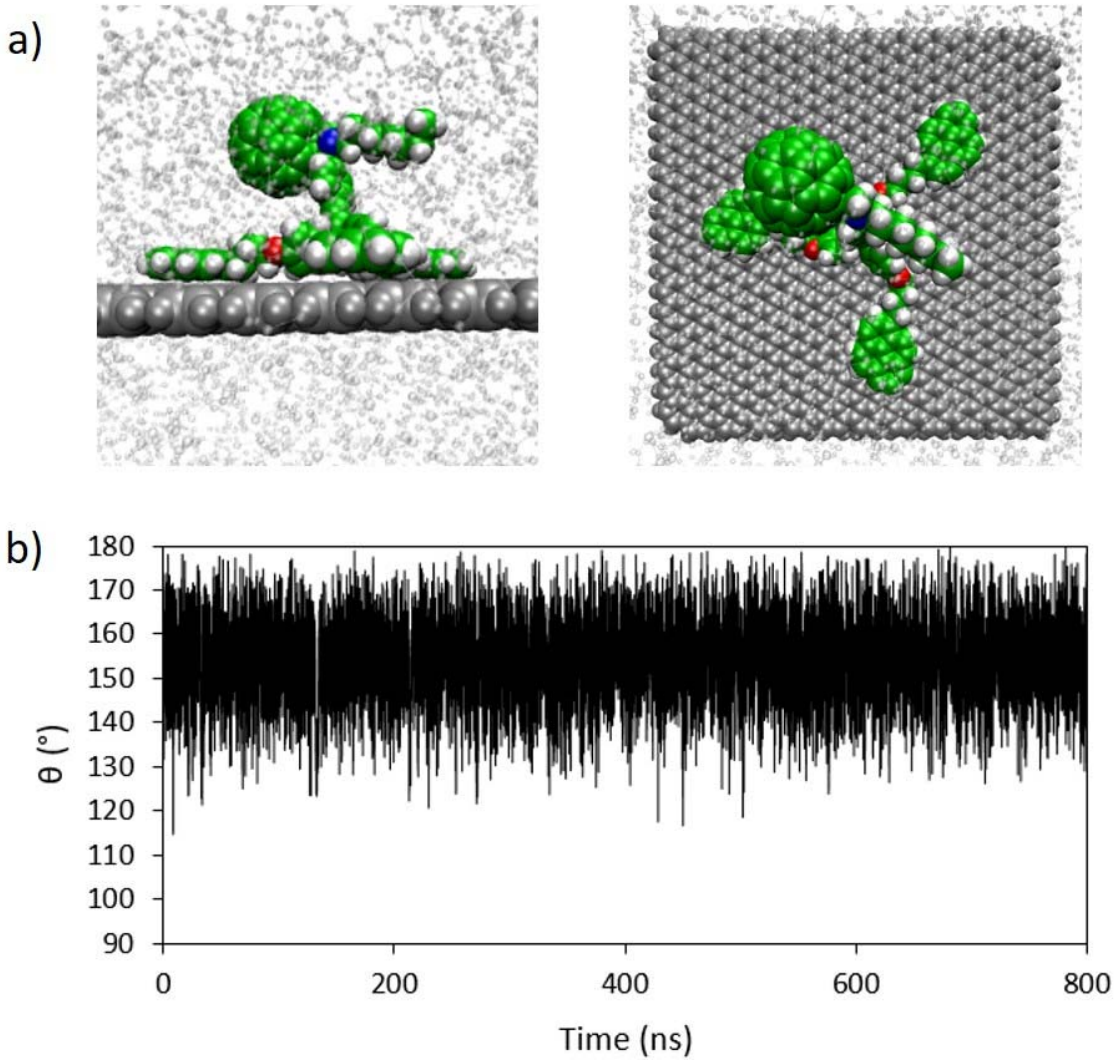

Figure S21. a) Side (left) and top (right) views of the initial structure used in the MM/MD simulation of the tripodal derivative **2** in a C_{60}–graphene non-interacting conformation in the presence of the solvent. b) Evolution along the 800 ns simulation time of the tilting angle θ, defined in Figure S14b, indicating the disposition of the C_{60} ball away from the graphene sheet.

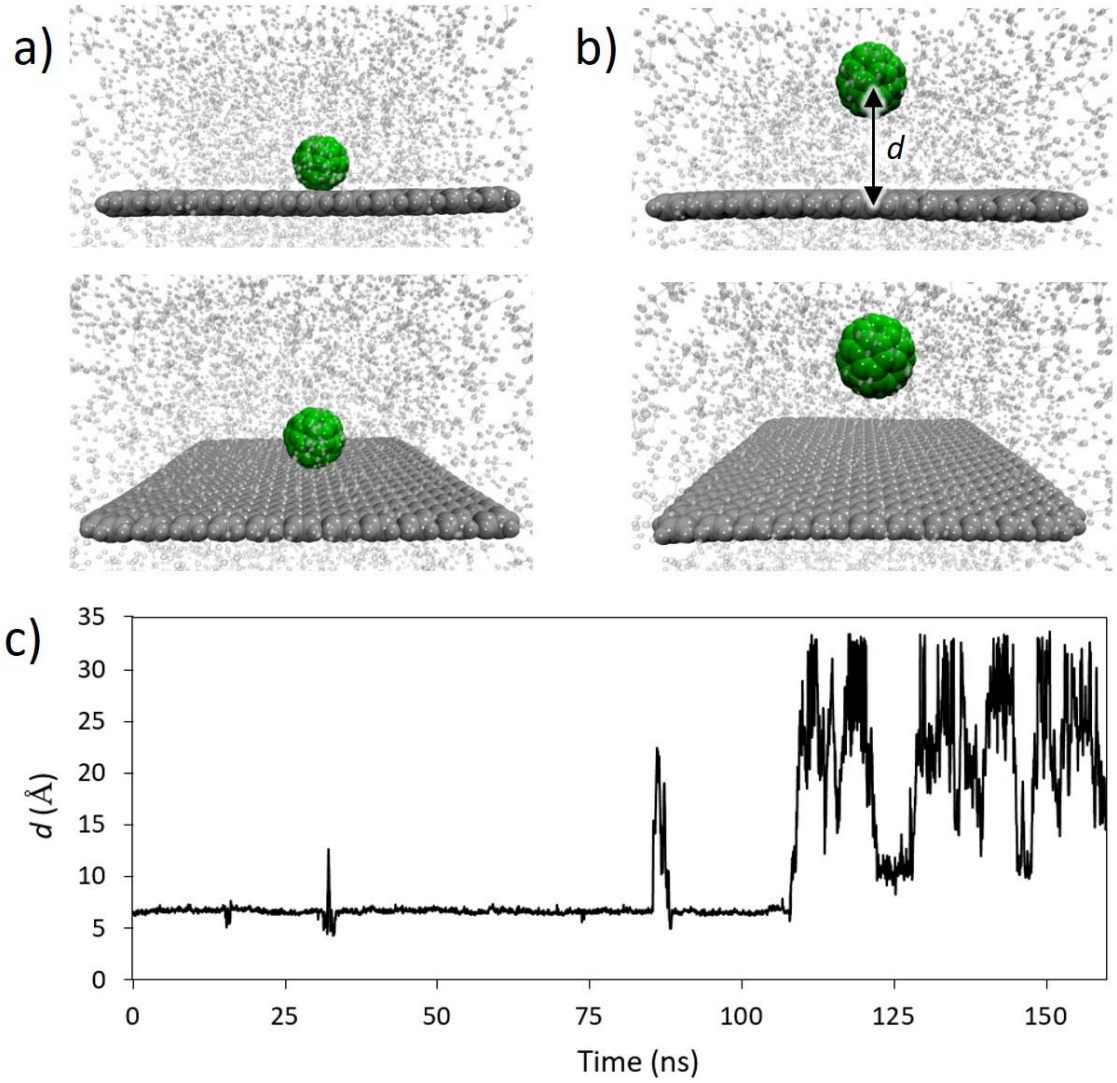

Figure S22. Representative snapshots of the two stages found in the MM/MD simulation of fullerene with graphene including explicit solvent molecules: a) C_{60} interacting with the graphene sheet, and b) C_{60} dissociated from the graphene layer and soaked into the solvent. c) Evolution of the distance between the fullerene centroid and the graphene sheet plane along the 160 ns simulation time.